REVIEW

Additive manufactured osseointegrated screws with hierarchical design

Wenbo Yang[1] · Hao Chen[1] · Haotian Bai[1] · Yifu Sun[1] · Aobo Zhang[1] · Yang Liu[1] · Yuchao Song[2,3] · Qing Han[1] · Jincheng Wang[1]

Abstract

Bone screws are devices used to fix implants or bones to bones. However, conventional screws are mechanically fixed with thread and often face long-term failure due to poor osseointegration. To improve osseointegration, screws are evolving from solid and smooth to porous and rough. Additive manufacturing (AM) offers a high degree of manufacturing freedom, enabling the preparation of predesigned screws that are porous and rough. This paper provides an overview of the problems currently faced by bone screws: long-term loosening and screw breakage. Next, advances in osseointegrated screws are summarized hierarchically (sub-micro, micro, and macro). At the sub-microscale level, we describe surface-modification techniques for enhancing osseointegration. At the micro level, we summarize the micro-design parameters that affect the mechanical and biological properties of porous osseointegrated screws, including porosity, pore size, and pore shape. In addition, we highlight three promising pore shapes: triply periodic minimal surface, auxetic structure with negative Poisson ratio, and the Voronoi structure. At the macro level, we outline the strategies of graded design, gradient design, and topology optimization design to improve the mechanical strength of porous osseointegrated screws. Simultaneously, this paper outlines advances in AM technology for enhancing the mechanical properties of porous osseointegrated screws. AM osseointegrated screws with hierarchical design are expected to provide excellent long-term fixation and the required mechanical strength.

Graphic abstract
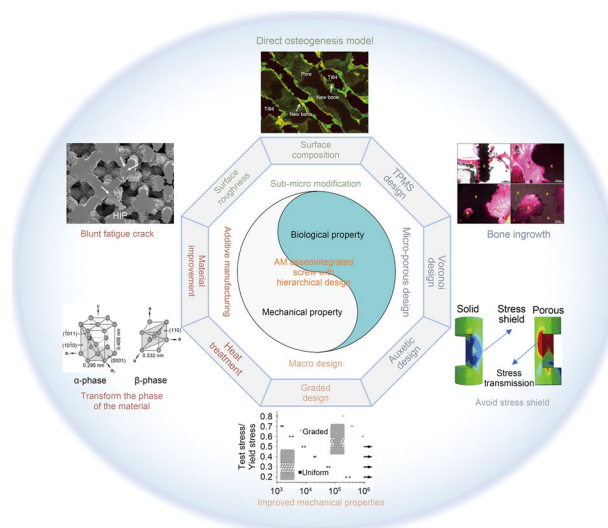
Introduction

Screws are widely used for implant- or bone-to-bone fixation in various clinical situations, including dental implants [1], arthroplasty [2], arthrodesis [3, 4], and fracture fixation [5]. Conventional screws are designed to improve screw–bone purchase by optimizing the profile, thereby increasing the holding force [6, 7]. For example, cancellous bone screws have deepened threads and reduced core diameters to achieve higher cancellous bone pullout strength [8]. Similarly, cortical bone trajectory screws enhance fixation in patients with osteoporosis by increasing the screw–cortical bone purchase [9]. In addition, increasing the length and diameter of a screw can improve the screw pull-out force [10–12]. These designs improve the initial fixation strength of screws. However, the dominant concept remains "mechanical fixation" whereas the proper integration of screw and bone is secondary, which does not solve the problem of screw loosening over the long term.

In the 1970s and 1980s, Brånemark et al. introduced the concept of osseointegrated dental implants to achieve long-term fixation through the osseointegration of screws [13, 14]. Osseointegrated screws are bone screws directly integrated at the screw–bone interface without other tissues [14, 15]. Before this, dental screws primarily possessed a smooth machined surface and were plagued by peri-screw bone loss [16]. Surface modification techniques are now widely used to create a robust interface between bone and screw by increasing the osteoblast activity on the screw surface. Changing the surface topography or surface chemistry is the most commonly used surface-modification strategy. The surface roughness of the screw increases the surface wettability while allowing an exponential increase in the cell attachment area, thereby improving the screw-bone osseointegration [17, 18]. In addition, some bioactive factors, such as bone morphogenetic protein-2 (BMP-2) [19, 20], bone morphogenetic protein-7 (BMP-7) [21], and the vascular endothelial growth factor [22], can be incorporated into screws through surface modification to achieve better osseointegration. Although surface-modification techniques can increase osteoblast activity on the screw surface and promote osseointegration, solid screws have no space for bone ingrowth. In addition, the stress-shielding effect, whereby solid screws with a high modulus of elasticity unload the mechanical load that the bone should support, leading to bone resorption, is considered a significant cause of long-term loosening [23, 24].

Porous screws have adjustable elastic moduli to avoid stress shielding and have open interconnected channels for bone ingrowth and vascularization [25, 26]. The ingrowth of bone into a porous screw provides mechanical interlocking between the bone and the screw. Studies show that this mechanical interlocking increases the pullout force of screws exponentially [27, 28]. In addition, some porous structures may be potential factors in improving the bone ingrowth ability of porous screws. A triply periodic minimal surface (TPMS) has a curvature similar to bone and a large surface area, facilitating bone ingrowth [29]. A Voronoi structure has randomness similar to the morphology of trabecular bone [30]. Porous screws with an auxetic structure expand under tension and resist pullout and shear in mechanics [31]. However, the mechanical properties of porous screws are inferior to those of solid screws.

Optimizing material distribution is an effective strategy to improve the mechanical strength of porous screws. The relatively dense portion of the gradient design provides mechanical strength, while the relatively porous portion provides space for the bone to grow into [26]. In addition, some emerging material optimization methods, such as topology optimization techniques, can increase the distribution of the material in the force concentration region to avoid screw breakage [32, 33].

Conventional manufacturing techniques employ turning, milling, or grinding of cylindrical bar stock to produce specific size screws [34]. However, manufacturing screws with 100 μm pores remains challenging. Other manufacturing techniques, such as the chemical vapor deposition [35], coagulant-assisted foaming [36], and vacuum diffusion bonding of titanium meshes [37], produce porous metals with good bone ingrowth capabilities. However, these porous-metal manufacturing techniques lack sufficient design–manufacturing flexibility (i.e., it is very difficult to manufacture porous screws based on a predesign). Additive manufacturing (AM), also known as three-dimensional (3D) printing, is a layer-by-layer predesigned numerical manufacturing method [38] and has natural advantages for manufacturing porous screws. However, AM technology also has certain drawbacks, mainly concerning the inability to precisely manufacture porous screws according to the predesign due to cracks in the substrates, which also reduce the mechanical strength of AM screws [39, 40]. Heat treatment can lead to a phase transformation in AM titanium screws and eliminate some manufacturing defects; this strategy is expected to improve the fatigue performance of the screws [41]. Further, β-titanium alloys have the advantage of a high strength-to-modulus ratio, which is expected to produce a new type of screw with low elastic modulus and high mechanical strength [42].

The profile design of traditional screws has been well summarized by Mudgal and Jupiter [6] and Shea et al. [7]. The burgeoning AM technology allows for the fabrication of high-quality porous metal implants, with potentially enormous implications for the development of screws [43, 44].

Wenbo Yang and Hao Chen have contributed equally to this work.

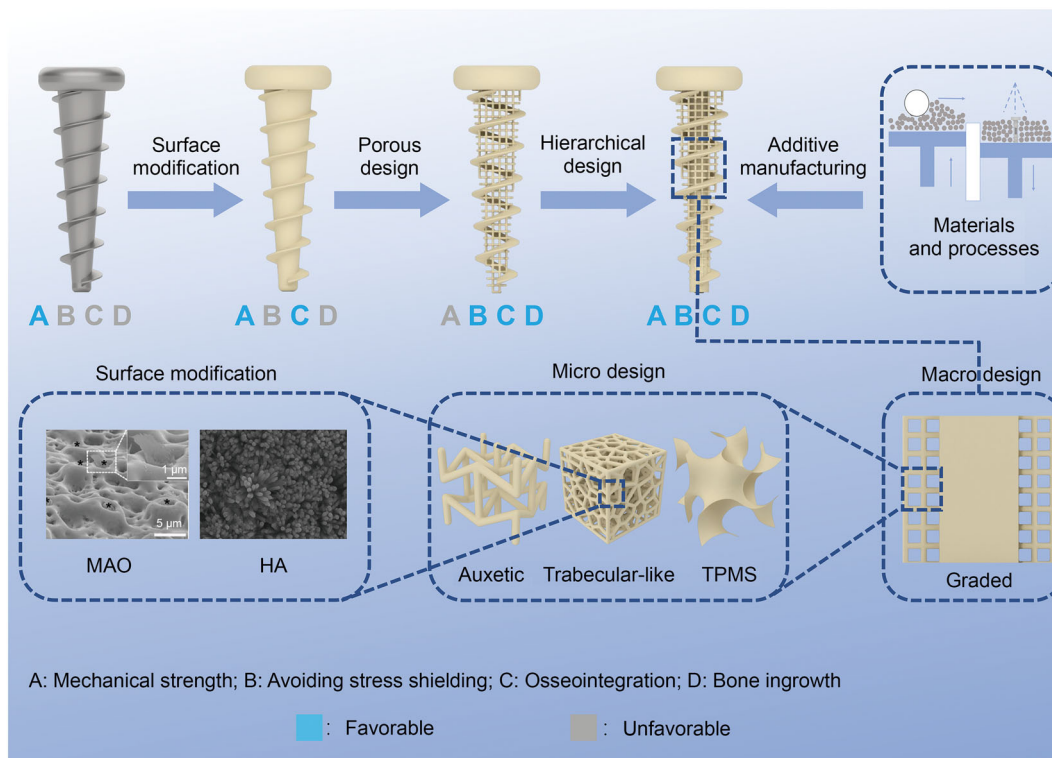Extended author information available on the last page of the article

Fig. 1 Schematic diagram of the development of bone screws

Agarwal et al. [44] reviewed various types of porous screws that simultaneously avoid the stress-shielding effect, allow the ingrowth of bone, and can be fabricated by AM technology. However, no review yet focuses on solutions to the main challenges faced by AM screws, namely, reduced mechanical performance and insufficient integration with bone. Thus, based on the above background, we summarize herein the concept of AM osseointegrated screws with hierarchical design, discussing macro design, micro design, surface modification, and the improvement of AM. This technology is expected to provide excellent long-term fixation and the required mechanical strength (Fig. 1).

From conventional solid screws to porous osseointegrated screws

Long-term loosening of conventional solid screws

Screw fixation is one of the most extensive fixation methods in clinical practice. The screw acts as a bridge, connecting two or more parts (bones, implants, and ligaments). However, bone screws often suffer from long-term loosening. In dentistry, a reduction in the height of the alveolar bone around a dental implant screw often occurs after implantation, which means that the screw loses its bone anchoring, affecting its survival in the oral cavity (Fig. 2a1) [45, 46]. In spinal

surgery, screws are widely used for joint fusion, including vertebral body fusion and sacroiliac joint fusion. However, peri-screw radiolucency is widely reported, suggesting bone resorption and pseudarthrosis (Fig. 2a3) [47–49]. In trauma surgery, radiolucency also occurs around the screws used for long-term fixation (Fig. 2a4). In total hip arthroplasty, screws are commonly used to fix the acetabular cup [40, 41]. Peri-screw radiolucency is also observed, which may reduce the fixation of the cup and lead to secondary surgery [50]. In anterior cruciate ligament reconstruction (ACLR), interference screws are widely used for fixation to provide stability and facilitate early and aggressive rehabilitation [51]. However, tunnel widening after ACLR has been widely reported clinically, resulting in clinical complications such as joint relaxation [52, 53]. In addition, bone resorption around screws can be reflected in the thinning of the surrounding cortical bone [23]. In more severe cases, a lagging cutout of the screw occurs (Fig. 2a2) [5].

Long-term loosening of conventional screws is mainly caused by bone resorption and poor integration of bone and screws. Several reasons can explain this phenomenon. First, the stress shielding effect can cause resorption of the surrounding bone, which is detrimental to bone regeneration [23, 54]. Second, solid screws lack space for bone ingrowth and transportation channels for bone growth material. The internal cavity of hollow screws lacks sufficient contact with bone tissue. Third, screws with smooth surfaces

Fig. 2 Long-term loosening of conventional solid screws and existing porous screws. **a** Long-term loosening of conventional solid screws. **a1** Decrease in height of the alveolar bone around the dental screw (Reproduced from [45], Copyright 2007, with permission from Wiley Periodicals, Inc.). **a2** Lagging cutout of screw at femoral neck (Reproduced from [5], Copyright 2004, with permission from Lippincott Williams). **a3** Peri-screw radiolucency in the vertebral body (Reproduced from [49], Copyright 2008, with permission from Lippincott Williams). **a4** Peri-screw radiolucency in the calcaneus (Reproduced from [71], Copyright 2019, with permission from the authors, licensed under CC BY). **b** Comparison of micro-computed tomography analysis and pull-out test for solid screws and porous screws (Reproduced from [59], Copyright 2019, with permission from the authors, licensed under CC BY). **c** Radiographs of porous screws. **c1** Radiograph of stemless total shoulder arthroplasty (Arthrex Inc., Naples, FL, USA) (Reproduced from [63], Copyright 2020, with permission from the authors, licensed under CC BY 4.0). **c2** Radiograph of osseointegrated dental screws (Trabecular Metal Implants, Zimmer Dental Inc., California, USA) (Reproduced from [72], Copyright 2017, with permission from Allen Press Inc.). **c3** Radiograph of the osseointegrated prostheses for the rehabilitation of amputees (OPRA, Integrum AB, Mölndal, Sweden) (Reproduced from [60], Copyright 2020, with permission from the authors, licensed under CC BY-NC-ND). **c4** Radiograph of additive manufacturing (AM) osseointegrated screw for sacroiliac fusions (iFuse-TORQ, SI-BONE, California, USA) (Reproduced from [3], Copyright 2022, with permission from the authors, licensed under CC BY-NC). **c5** Radiograph of porous screw cages (reproduced from [73], Copyright 2016, with permission from Korean Society of Spine Surgery). **d** Existing porous screws. **d1** Photograph of stemless total shoulder arthroplasty systems (Arthrex Inc., Naples, FL, USA) (Reproduced from [62], Copyright 2018, with permission from the authors,

licensed under CC BY 4.0). **d2** Photograph of osseointegrated dental screws (Trabecular Metal Implants, Zimmer Dental Inc., California, USA) (Reproduced from [35], Copyright 2013, with permission from the authors, licensed under CC BY-NC-ND). **d3** Photograph of OPRA (Integrum AB, Mölndal, Sweden) (Reproduced from [23], Copyright 2021, with permission from the authors, licensed under CC BY-NC-ND). **d4** Photograph of AM osseointegrated screw for sacroiliac fusions (iFuse-TORQ, SI-BONE, California, USA) (Reproduced from https://si-bone.com/providers/solutions/pelvic-trauma/ifuse-torq, with permission from SI-BONE). **d5** Photograph of AM osseointegrated screw for sacroiliac fusions (3D Printed implants, Genesys SIros™, Texas, USA) (Reproduced from https://www.genesysspine.com/products/sacral/lateral-sacroiliac-joint-fusion-siros-3d-printed/, with permission from Genesys). **d6** Photograph of AM osseointegrated screw for sacroiliac fusions (3D™ SI Joint Fusion System, Cornerloc TransLoc, Oklahoma, USA) (Reproduced from https://cornerloc.com/transloc-3d/, with permission from Cornerloc). **d7** Photograph of AM osseointegrated screw for sacroiliac fusions (FIREBIRD SI Fusion System, Orthofix, Texas, USA) (Reproduced from https://orthofix.com/products/spine-solutions/spine-procedures/si-fusion/firebird-si-fusion-system/, with permission from Orthofix). **d8** Photograph of AM osseointegrated pedicle screw (Bi-Cortical/Mid-Line Porous Cannulated screw, Tsunamimedical, Ventotene, Italy) (Reproduced from https://www.tsunamimedical.com/product-category/spine/pedicle-screw-systems/modular-pedicle-screw-shafts/, with permission from Tsunamimedical). **d9** Photograph of AM osseointegrated pedicle screw (Porous Cannulated screw, Tsunamimedical, Ventotene, Italy) (Reproduced from https://www.tsunamimedical.com/product-category/spine/pedicle-screw-systems/modular-pedicle-screw-shafts/, with permission from Tsunamimedical)

lack sufficient initial stability after implantation, and excessive micro-movement may lead to the formation of fibrous tissue around the screws [55, 56]. Fourth, a smooth surface is not conducive to the adhesion and proliferation of bone cells [17, 57]. AM porous screws possess an open porous structure and a rough surface, which allows bone ingrowth that interlocks the bone and screw [58]. In addition, porous screws can automatically collect autologous bone during screwing, thus accelerating healing. Micro-computed tomography analysis indicates good ingrowth of bone into porous screws. The bone ingrowth significantly strengthens the fixation of porous screws with respect to solid screws, as demonstrated by pullout tests (Fig. 2b) [59].

Commercially available porous bone screws

Currently, porous screws have been clinically validated for fixing implants to bone and for fixing bone to bone, although some screws are not produced by AM techniques (Table 1).

A porous screw used to fix an implant to bone is integrated into the bone at one end and connected to the foreign implant by mechanical fixation at the other end. A well-osseointegrated porous screw corresponds to the "root" of the implant in the bone. Inspired by Brånemark, osseointegrated screws are applied in osseointegrated prostheses for the rehabilitation of amputees (OPRA; Figs. 2c3 and 2d3) [23]. The OPRA instrument (Integrum AB, Mölndal, Sweden) consists of three parts: an abutment screw, an abutment, and an osseointegrated screw, the so-called "fixture" [60]. Compared with socket prostheses, the OPRA improves patients' quality of life and limb function [61]. Stemless total shoulder arthroplasty (Arthrex Inc., Naples, FL, USA) is also designed with osseointegrated screw fixation, which consists of three parts: an anatomical humeral head, a trunnion for epiphyseal fixation, and a hollow cage screw for metaphyseal fixation (Figs. 2c1 and 2d1) [2, 62]. Prostheses with a hollow screw design preserve bone volume and reduce bone resorption more than traditional shoulder prostheses do [62, 63]. In addition, dental screws pioneered the development of osseointegrated screws (Trabecular Metal Implants, Zimmer Dental Inc., California, USA) with a porous trabecular design, which achieved good clinical results (Fig. 2c2 and 2d2) [64]. Histological sections show that copious bone growth penetrates into the porous trabecular portion [65]. Although this highly porous tantalum trabecular material was produced by chemical vapor deposition rather than AM, the good clinical results validated the feasibility of this design [35].

Osseointegrated porous screws can also fix two bones, as in arthrodesis. Classical sacroiliac fusions are often performed with porous-coated triangular titanium implants (SI-BONE, Inc., San Jose, CA, USA) [66, 67]. Clinical reports also show similarly good fusion results with hydroxyapatite-coated slotted screws (Globus Medical Inc.,

Audubon, Pennsylvania, USA) [68]. Recently, many systems are developing versions of a threaded, 3D-printed bone screw for this application (SI-BONE, Genesys Siros, Cornerloc Transloc, Orthofix Firebird SI) (Figs. 2d4–2d7). Two patients used this AM porous screw (iFuse-TORQ, SI-BONE) and experienced complete relief of pain (Fig. 2c4) [3]. In addition, various promising standalone threaded titanium-alloy cylindrical screw cages were used for interbody fusion of the lumbar spine in the mid-1990s (Fig. 2c5) [69, 70]. However, without the aid of pedicle screws for fixation, this independent threaded cage lacked sufficient stability and was phased out. As shown in Fig. 2a3, pedicle screws face the same problem of distant loosening. More recently, Tsunamimedical introduced additively manufactured porous pedicle screws (Ventotene, Tsunamimedical, Italy) to promote osseointegration of the screws (Figs. 2d8 and 2d9). Currently, there are no clinical reports on the use of such pedicle screws.

To deal with these problems, we propose the concept of hierarchically designed AM osseointegrated screws and summarize the progress in surface modification, micro design, macro design, and AM for this concept.

Potential problems faced by porous bone screws

Although porous screws have many advantages, which are thoroughly discussed above, they also face potential problems, including inadequate osseointegration and concerns about mechanical strength.

First, the combination of screw and bone is inadequate, and the long-term fixation of screws can still be improved. Optimizing the porous structure is considered a potential facilitator of bone ingrowth, which needs further exploration [23, 29]. In addition, although the bone grows into the porous screw, a gap remains between the bone and the porous screw substrate [18, 76]. Surface modification allows the bone to be integrated directly into the substrate surface of the porous screw without gaps [77].

Second, the mechanical properties of porous screws also deserve full attention. Screws are subjected to complex loads during and after implantation, including torsion, compression, tension, and bending (Table 2). In addition, because a screw is subjected to cyclic loading, fatigue resistance is essential for improving the screw lifetime. Broken screws cause serious clinical complications, and both defects in AM and porosity decrease screw strength. The mechanical strength of screws should be improved by improving the micro and macro design and the AM technology of screws.

To deal with these problems, we propose the concept of hierarchically designed AM osseointegrated screws and summarize the progress in surface modification, micro design, macro design, and AM for this concept.

Table 1 Summary of literature on clinically available porous screws

Application	Research type	Number of patients	Follow-up (in months)
Dental screw [1]	Case report	1	12
Dental screw [65]	Clinical-histologic case report	1	4
Dental screw [72]	Retrospective study	42	25
Dental screw [64]	Prospective study	30	60
OPRA [74]	Retrospective study	51	60
OPRA [61]	Prospective study	51	24
Shoulder arthroplasty [63]	Retrospective study	39	24
Shoulder arthroplasty [75]	Prospective study	49	108
Shoulder arthroplasty [62]	Prospective study	73	58
Sacroiliac fusions [3]	Case report	2	
Sacroiliac fusions [68]	Prospective study	32	24
Interbody fusion [73]	Retrospective study	45	240

OPRA: osseointegrated prostheses for the rehabilitation of amputees

Table 2 Mechanical properties required for bone screws

Mechanical property	Test method	Test indicators	Related standards	References
Shear resistance	Torsional test	Torque	ASTM F543	[59, 78]
		Torsional strength	ISO 6475	
			BS 3531–5.6–1991	
Bending resistance	Three-point bending test	Bending strength	YY/T 0119.5–2014	[59, 78]
Tensile resistance	Tensile testing	Tensile strength		[31]
Compression resistance	Compression test	Compression strength		[26, 79]
Fatigue resistance	Fatigue testing	Fatigue strength/ cycle number	YY/T 0119.5–2014	[26, 80]

Surface modification of additive-manufactured osseointegrated screws

The surface roughness of the screw is a critical factor affecting osseointegration. One of the characteristics of AM screws is the numerous semi-molten powders, tens of microns in diameter, attached to their surface. On the one hand, the rough surface created by these powders was considered to be an advantage over conventional smooth screws (Figs. 3b and 3e) [81]. Cells usually form numerous pseudopods on this rough surface, indicating good adhesion [82]. A considerable amount of bone tissue remains on the surface of AM screws after push-out tests, indicating a higher osseointegration rate and bonding strength than conventionally machined screws. Histological sections also show more active osteogenesis around the rough surface of the AM screw than is the case with conventional smooth screws [81]. On the other hand, the loosely bonded powders constitute foreign bodies when shed in the body and may cause chronic inflammation and osteolysis [83, 84]. Song et al. [85] categorized these unmelted powders as either harmful or valuable powders. Powders with a contact angle θ greater than 90° with the scaffold matrix are harmful powders and are more likely to fall off the scaffold matrix after implantation in the body. These powders can be removed by surface modification techniques, such as acid etching or sandblasting [85, 86]. Powders with a contact angle less than 90° are defined as valuable powders, providing surface roughness. Although AM screws have a rough surface, this roughness is on the order of ten microns.

Titanium-based materials are well known for in vivo stability and corrosion resistance provided by the natural oxide film that forms on their surface. However, this also means biological inertness, which hinders osseointegration and bone conductivity. Without surface modification, bone formation in porous titanium screws forms a distance pattern, which means that bone forms only around the strut, not directly on the strut surface [77, 87]. Surface modification changes the
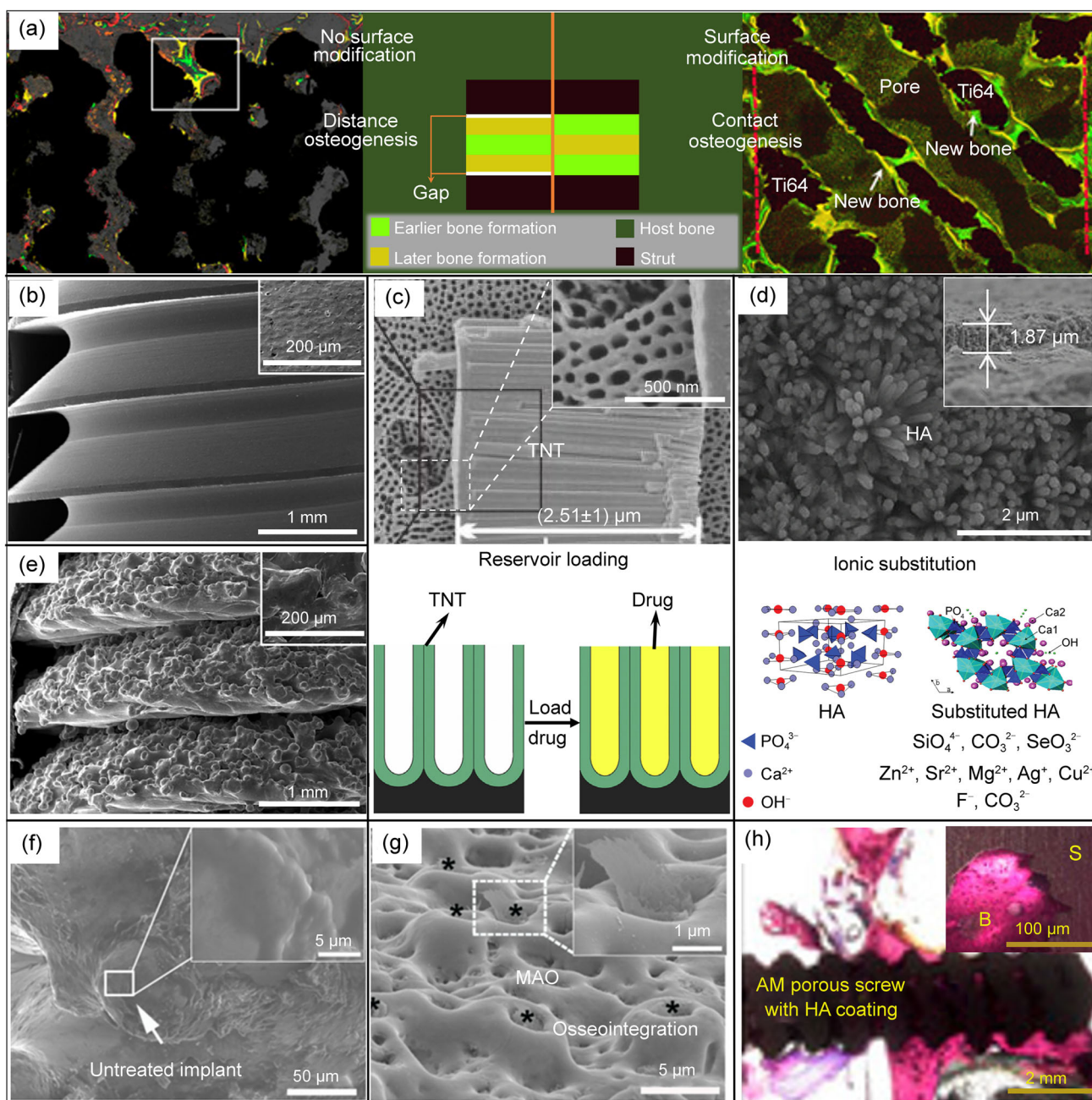
Fig. 3 Surface modification of additive manufacturing (AM) osseointegrated screws. **a** Schematic diagram and fluorescence image of two modes of osteogenesis. Porous scaffolds without surface modification are in distance osteogenesis mode (left) (reproduced from [87], Copyright 2018, with permission from Elsevier Ltd.), whereas porous scaffolds with surface modification are in contact osteogenesis mode (right) (reproduced from [77], Copyright 2016, with permission from American Chemical Society). **b**, **e** Scanning electron microscopy (SEM) images showing the smooth surface and rough surface of screws machined conventionally and by electron beam melting, respectively (reproduced from [81], Copyright 2020, with permission from Elsevier B.V.). **c** Anodizing and its further functionalization (the lower part is reproduced from [91], Copyright 2019, with permission from Elsevier; the upper part is reproduced from [110], Copyright 2020, with permission from Elsevier). TNT: TiO$_2$ nanotube **d** Hydroxyapatite (HA) coating and its further functionalization (the lower part is reproduced from [101], Copyright 2020, with permission from The Royal Society of Chemistry; the upper part is reproduced from [111], Copyright 2019, with permission from The Chinese Society for Metals (CSM) and Springer-Verlag GmbH Germany, part of Springer Nature). **f** SEM images showing no ruptured bone tissue attached to the untreated implant surface. **g** SEM images showing ruptured bone tissue attached to the micro-pits of the microarc oxidation (MAO)-treated implant (**f** and **g** reproduced from [77], Copyright 2016, with permission from American Chemical Society). **h** Stained histological sections of AM porous screws with HA coating, showing good bone ingrowth and osseointegration (reproduced from [97], Copyright 2020, with permission from the authors, licensed under CC BY 4.0)

osteogenesis pattern to contact osteogenesis, which means that bone forms directly on the surface of the porous screws (Fig. 3a) [77]. Furthermore, the screws can be functionalized by advanced modifications based on primary surface modifications.

Primary surface modification of additive-manufactured osseointegrated screws

Surface modification can create different roughness scales on the surface of AM porous screws to improve integration with the bone [18]. For example, microarc oxidation (MAO), also known as plasma electrolytic oxidation, can create micron-level orange-peel-like surface morphology on titanium substrates (Fig. 3g) [77, 88]. Scanning electron microscopy (SEM) images show that bone interlaces with 1- to 2-μm-diameter micro-pores formed by MAO, whereas the surface of the untreated AM porous scaffold lacked bone attachment (Figs. 3f and 3g). Push-out tests also show that the biofixation strength of the MAO-treated AM porous scaffold significantly exceeds that of the AM porous scaffold [77]. Anodization produces uniform and regular TiO$_2$ nanotubes (TNTs) on the surface of porous titanium alloys, which means nano-scale surface roughness and a higher surface-to-volume ratio (Fig. 3c). Changing the anodization voltage can generate TNTs of different diameters on the screw surface [89] into which pseudopods of osteoblasts can grow directly [90, 91]. Compared with the AM group, the new bone tissue in the anodized group is tightly bound to the Ti–6Al–4V matrix with a larger area, and no obvious fibrous connective tissue interface layer forms between the implant and bone in the anodized group, indicating the direct fusion of the implant with the bone tissue [18]. Changes in surface topography transmit signals to cells through integrins, which further affects the biological behavior of bone cells [92]. Surface topography can also polarize macrophages in the M2 direction through a paracrine pathway, forming an anti-inflammatory microenvironment conducive to bone repair and reconstruction [93].

Changes in surface composition are another reason for improving the osseointegration of AM screws. For example, MAO or anodic oxidation can alter the charge on the surface of AM screws [88, 94]. The charged surface attracts charged fibronectin molecules and osteoblasts, which is thought to be the first step in osseointegration after implantation into the body [94]. In addition, the change in surface charge accelerates the deposition of hydroxyapatite (HA), one of the main inorganic components in native bone. Anions attract calcium ions, which in turn attract phosphate ions to form HA precipitates on the surface [18, 95]. HA can also be added directly onto the screw surface as a coating to enhance the osseointegration of the screw (Fig. 3d) [5, 68]. Histological sections taken from patients demonstrate the tight bond between the HA-coated screw and bone [96]. Huang et al. [97] reported an HA-coated AM porous bone screw. Histological sections show that the bone grows sufficiently into the pore and integrates well with the matrix of the porous screw (Fig. 3h).

Advanced surface modification of additive-manufactured osseointegrated screws

After the primary surface modification discussed above, further bioactive factors can be added to functionalize the bone screws. In addition to the excellent capacity for osseointegration of TNT, its tubular structure may serve as a drug reservoir for local drug delivery, which avoids adverse reactions caused by systemic administration (Fig. 3c). Lee et al. [98] loaded the recombinant human bone morphogenetic protein-2 (rhBMP-2), a cytokine that induces bone formation, into TNTs on the screw surface to promote the screw–bone integration and avoid the risk of heterotopic ossification caused by the systemic application of rhBMP-2. He et al. [91] loaded 1α,25-Dihydroxyvitamin D3 (VD3), a vitamin that can promote osteoblast and osteocyte maturation, into TNTs on the surface of a porous titanium scaffold. In vivo and in vitro evaluations show that osseointegration improves significantly. In addition to organic matter, TNTs can be doped with inorganic matter to promote bone formation. Zhao et al. [99] developed screws with Si–TiO$_2$ nanotubes through Si plasma immersion ion implantation. Si–TiO$_2$ nanotubes offer better pre-osteoblast adhesion, greater proliferation, and more facile extracellular matrix deposition than TNTs, and have a greater pull-out force. In addition, TNTs can be doped with antibacterial substances. Xiang et al. [100] used a hybrid-surface system to extend the duration of drug release of vancomycin-loaded TNT capped by folic acid-functionalized ZnO, which remains stable in physiological environments but releases Zn^{2+} and vancomycin in mildly acidic environments after bacterial infections. At the same time, due to the folic acid and the sustained release of Zn ions, this hybrid-surface system offers excellent biocompatibility.

Based on the HA coating, substituted-HA coatings (Fig. 3d) are attracting research interest because they provide screws with additional properties, such as osteoinduction or antibiotic activity, which accelerates biomechanical fixation and hinders infection and osteoporosis [101]. Different ions can replace both the cation and anion of HA for different purposes. Different cations, including Mg^{2+} for enhancing bioactivity properties, Ag$^+$ for enhancing antibacterial properties, can substitute for Ca^{2+} in substituted-HA coatings [102, 103]. For example, zinc-substituted HA has been studied for stimulating bone formation and antibacterial properties [104, 105]. Similarly, different anions, including SiO$_3{}^{2-}$, F$^-$, and CO$_3{}^{2-}$, can also be applied in substituted-HA coatings by replacing OH$^-$ or PO$_4{}^{3-}$ [106, 107]. For example, fluoride-substituted HA improves the bonding

strength and reduces the dissolution rate [107]. What's more, co-substitution (i.e., combining two or more substituents that lead to synergistic, complementary, or compensatory effects) is a brilliant strategy to optimize HA coatings [108]. Recently, combining substituted HA with nanostructures provided novel ideas for orthopedic coatings, including how to improve biocompatibility, corrosion resistance, and the mechanical properties of the coatings [109]. These research efforts require more in vivo experiments to verify their safety.

In conclusion, surface modification endows AM porous screws with sub-microscopic designed surfaces, resulting in stronger bone–screw interfaces while reducing fabrication time and improving the fixation.

Micro-design of additive-manufactured osseointegrated screws

Surface designs are mainly on the scale of nanometers to microns, whereas micro designs are on the scale of microns to millimeters, allowing bone to grow into and thus interlock with AM porous screws. The mechanisms involved are multifaceted. From a mechanistic perspective, the porous structure avoids the stress-shielding effect (Fig. 4a). From a biological perspective, porous screws provide a 3D network, which promotes the proliferation and differentiation of bone marrow mesenchymal stem cells, guides bone regeneration, and promotes nutrient diffusion. The study of Yin et al. shows that the expression of osteogenesis-related genes in the porous group is significantly greater than that in the flat group [112]. Staining by 5-ethynyl-2'-deoxyuridine also indicates that the porous group promotes cell proliferation. Furthermore, the porous structure guides the bone-regeneration process. At the tissue level, the orientation of collagen fibers, acting as a secondary template for cell deposition and supporting the growth of bone into the scaffold, is also guided by porous scaffolds [24]. At the cellular level, the cytoskeleton is guided by a porous structure, as observed by staining for F-actin [112]. At the molecular level, mechanical transduction, such as pathways related to yes-associated protein, may mediate this biological process [113]. The greater expression of yes-associated protein at gene and protein levels in the porous group than in the flat group was observed by using quantitative polymerase chain reaction (qPCR) and immunofluorescence staining [112]. Thus, porous screws improve long-term fixation.

The mechanical strength of porous screws is also closely related to the microporous design. Hedayati et al. [114] reported that, for a porous structure composed of truncated-cube unit cells, the ratio of the inclined strut length to the uninclined strut length strongly affects the elastic modulus and Poisson's ratio. The deformation mechanism of the porous structure, which is related to mechanical properties

such as fatigue performance, also depends strongly on the pore shape [115]. The micro-design parameters of porous osseointegrated screws mainly include the porosity, pore size, and pore shape, and affect both the mechanical and biological properties of these screws. Novel pore architectures, such as the Voronoi, TPMS, and auxetic structures, have attracted more attention due to their unique properties.

Porosity and pore size of additive-manufactured osseointegrated screws

Porosity and pore size are critical parameters in the design of porous screws, significantly affecting the mechanical properties and biological performance of porous screws. Porosity is defined as the percentage of pore space in a solid and can be expressed by [116]

$$\rho_{\text{relative}} = \frac{\rho_{\text{structure}}}{\rho_{\text{material}}}, \tag{1}$$

$$P = (1 - \rho_{\text{relative}}) \times 100\%, \tag{2}$$

where $\rho_{\text{structure}}$ is the mass-to-volume ratio of the porous sample, ρ_{material} is the density of the solid material, ρ_{relative} is the relative density of the porous sample, and P is the porosity of the porous sample. The 3D definition of pore size is the diameter of the largest virtual sphere in the structure [117]. For porous structures composed of repeating arrays of identical units, such as a TPMS, the unit size is used to describe the pore size [38].

Effect of pore size and porosity on mechanical properties of additive-manufactured osseointegrated screws

Porosity usually correlates negatively with mechanical properties. The three-point bending and torsion tests reveal a higher mechanical strength of porous screws with low porosities [59, 78]. Compression and tensile fatigue tests show that fatigue life also correlates negatively with porosity [118]. According to the mechanics of the materials, the mechanical properties of the porous structures, including the elastic modulus and yield strength, depend on their relative densities [119]. A power-law relationship exists between the mechanical properties (i.e., elastic modulus E and yield strength) of the porous structure and its relative density (Fig. 4b) [40, 120, 121]. Other studies report a linear dependence of mechanical properties on porosity [122, 123]. This phenomenon may be related to the deformation mechanism of the porous structure. The mechanical properties are linear in relative density in the tensile-dominated deformation mode, while the bending-dominated deformation mode follows a power-law relationship [115, 124]. In conclusion, low-porosity screws
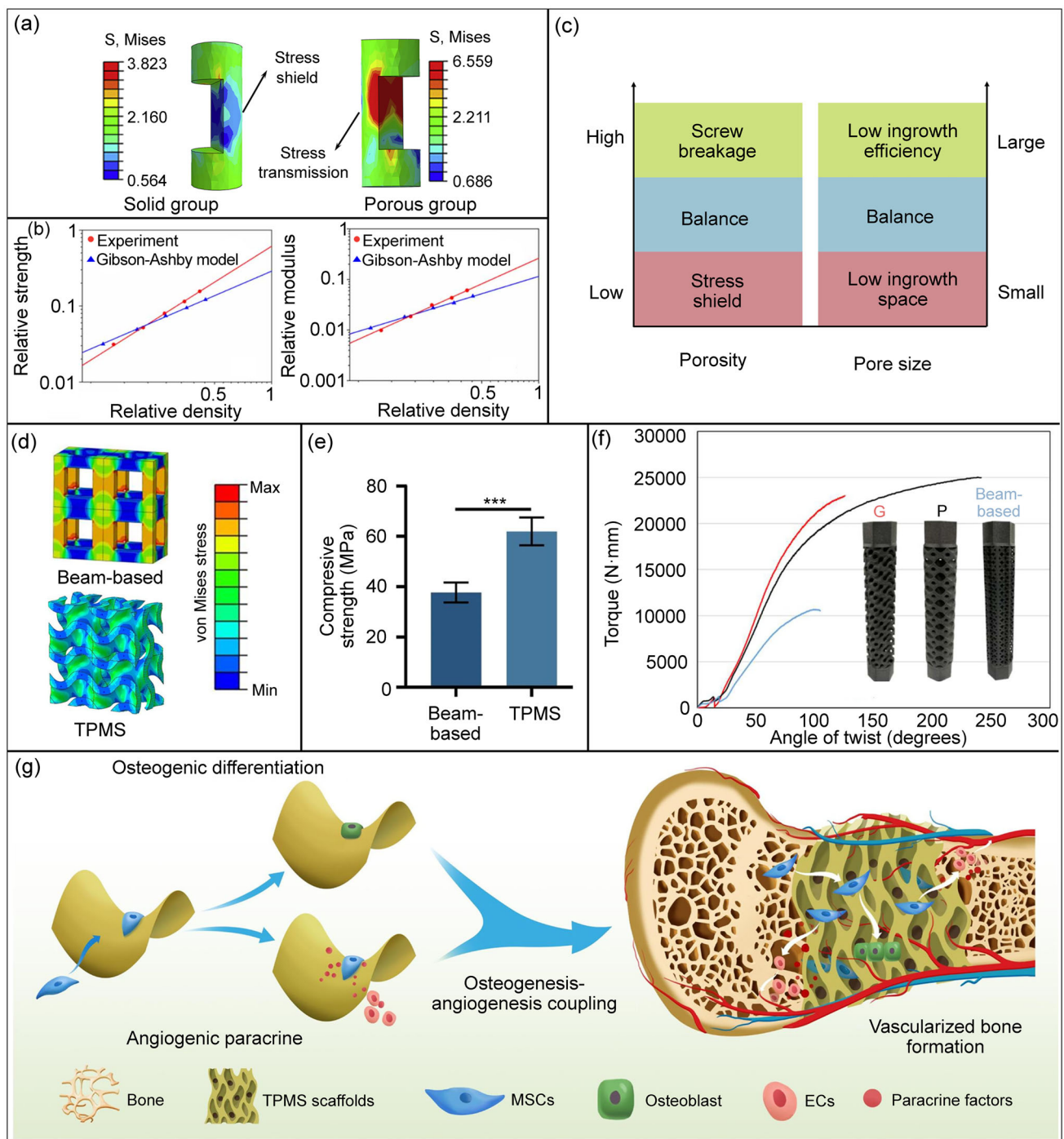
Fig. 4 Porosity, pore size, and triply periodic minimal surface (TPMS) design of additive manufacturing (AM) osseointegrated screw. **a** Porous structure avoids the stress-shielding effect (reproduced from [27], Copyright 2019, with permission from the authors, licensed under CC BY-NC-ND). **b** Relationship between mechanical strength and porosity (reproduced from [40], Copyright 2020, with permission from IOP Publishing Ltd). **c** Effect of pore size and porosity on the mechanical and biological properties of screws. **d** Finite-element analysis of beam-based and TPMS scaffolds, showing no stress concentration in TPMS (reproduced from [29], Copyright 2022, with permission from the authors, licensed under CC BY 4.0). **e** Compressive strength of beam-based scaffold and TPMS scaffold (reproduced from [29], Copyright 2022, with permission from the authors, licensed under CC BY 4.0). **f** The torque of beam-based scaffold and TPMS scaffold (reproduced from [149], Copyright 2022, with permission from the authors, under exclusive licence to Springer-Verlag London Ltd., part of Springer Nature). **g** Schematic diagram showing how TPMS affects bone regeneration (reproduced from [29], Copyright 2022, with permission from the authors, licensed under CC BY 4.0). MSCs: mesenchymal stem cells; ECs: endothelial cells

have higher mechanical strength and a lower risk of breakage than high-porosity screws.

In general, the mechanical properties of porous metal screws depend on their overall porosity, but they are also affected by pore size. Some reports state that the mechanical properties decrease with increasing pore size. For instance, the study of Yang et al. shows that the elastic modulus and compressive yield strength decrease with increasing unit size [125]. Ran et al. [126] fabricated porous Ti_6Al_4V implants with pore dimensions of 400, 600, and 800 μm and a wall thickness of 300 μm. Their results show that the mechanical properties decrease with increasing pore size, which is attributed to a porosity that correlates positively to the pore size for a given wall thickness. However, some researchers reported different results when the predesigned porosity was fixed. Taniguchi et al. [127] used selective laser melting (SLM) to manufacture three porous titanium implants with an intended porosity of 65% and pore sizes of 300, 600, and 900 μm, and reported that the mechanical properties decrease with decreasing pore size. This phenomenon is attributed to the powder used for AM having a certain diameter and to the powder on the surface not completely melting during manufacturing. Due to the manufacturing mismatch, for a given porosity, the mechanical properties are degraded for smaller pore sizes, slimmer walls, and a greater fraction of the unmelted part of the wall [127]. As the pore size approaches the printable threshold, the adhesion between the powders and the mechanical strength decrease, mainly due to the limitations of manufacturing technology [128].

Effect of pore size and porosity on biological properties of additive-manufactured osseointegrated screws

In contrast with the mechanical strength, low porosity does not improve the biological properties of porous screws (Fig. 4c). A decrease in porosity causes the elastic modulus of the screw to exceed that of the bone, leading to stress shielding, which means that screws with a high elastic modulus offload the mechanical load the bone should bear, resulting in bone resorption and detrimental bone regeneration. When the porosity is close to zero, the elastic modulus of metals (Ti_6Al_4V: 110 GPa; CoCrMo alloys: 210 GPa [43, 126]) is much higher than that of trabecular bone (from 0.07 to 6.9 GPa [129–131]) and cortical bone (from 3 to 40 GPa [40, 43, 131]). Studies show that when the stress of the surrounding bone tissue is between 20 and 60 MPa, the surrounding bone tissue is in a state of active reconstruction [132]. The bone around solid screws experiences less stress. Fortunately, the elastic modulus of porous screws can be controlled by the porosity. Studies show that titanium alloys with 60%–80% porosity have elastic moduli similar to bone (1–8 GPa), which avoids stress shielding and enhances osseointegration [38, 82, 133].

Higher porosity also means higher permeability and more space for bone ingrowth and vascularization [134]. Higher permeability means better mass transport (the ability of cells to enter and migrate into the scaffold and the ability of oxygen, nutrients, and waste to diffuse through the scaffold). In addition, the study of Cheng et al. [135] shows that the vascular endothelial growth factor increases with increasing porosity, indicating that high porosity induces vascularization to support bone ingrowth. Pei et al. [40] implanted 58%–85% porosity scaffolds into rabbits and beagle dogs and used push-out experiments to measure the stability between the scaffold and the bone. One month after implantation, the scaffolds' shear strength with 58%, 73%, and 85% porosity was 48, 55, and 60 MPa, respectively, indicating that higher porosity promotes early osseointegration.

However, higher porosity does not mean the best fixation. Kelly et al. [38] showed that, although high-porosity (90%) implants have more bone ingrowth, they do not have higher bone–implant shear strength. The maximum force, energy to failure, and shear strength peaked between 60% and 70%. The optimum porosity reported by other studies is similar. Chen et al. [136] used SLM to manufacture scaffolds with 60% and 70% porosities and performed in vivo and in vitro experiments. The results show that a scaffold with 60% porosity strongly promotes cell proliferation, osteogenic differentiation, and bone ingrowth. Pei et al. [40] conducted push-out experiments six months after implanting the scaffolds with 58%–85% porosities. All test specimens broke in the mature bone area rather than in the bone-formation area, indicating that 58%–85% porosity is suitable for osseointegration. Shah et al. [137] used Raman spectroscopy and electron microscopy to investigate the ultrastructure of the bone–implant interface of solid and porous implants with a porosity of 62.7%. The carbonate-to-phosphate ratio, phenylalanine, and tyrosine levels of bone healing at the implant interface with 62.7% porosity were more similar to native bone, indicating that this porosity was expected to reduce the stiffness mismatch between the screw and bone, eliminating the stress shielding effect. These studies suggest that controlling the porosity to 60%–80% promotes the long-term fixation of porous screws.

Pore size also profoundly affects biological performance, including the invasion of cells and the ingrowth of bone. On the one hand, screw pores form the spatial basis for bone ingrowth, and a pore that is too small is not conducive to bone ingrowth (Fig. 4c). Human trabecular bone is between 100 and 200 μm thick, depending on the part of the bone [138]. Theoretically, to meet the needs of bone ingrowth, screw pore size should not be less than this range. Hulbert et al. [139] showed that 75–100 μm pores lead to the ingrowth of unmineralized bone-like tissue, whereas smaller pores (10–44 and 44–75 μm) only had infiltration of fibrous tissue. Existing fabrication techniques also limit the minimization of pore

size. Pores that are too small may be blocked by unmelted powders and become solid [128].

Moreover, permeability (a parameter that predicts the ability of cells and nutrients to diffuse deep into the scaffold) increases as the pore size increases [128]. Screws with small pore sizes are not conducive to bone ingrowth due to limited space, nutrients, and oxygen supplements. Many studies confirm that pores that are too small are not conducive to fixing screws in bone. Chang et al. [37] used vacuum diffusion bonding to prepare porous titanium with a porosity of 70% and an average pore diameter of 188–390 μm. The results show that the porous scaffold with an average pore size of 390 μm was more favorable for cell proliferation and bone ingrowth than scaffolds with smaller pore sizes. Taniguchi et al. [127] implanted porous titanium scaffolds with a porosity of 65% and pore sizes of 300, 600, and 900 μm into a rabbit femur for two, four, and eight weeks. At all time points, those with 600 μm pores fixate better than those with 300 μm pores. Similar results were obtained by Ran et al. [126]: after implanting 400, 600, and 800 μm scaffolds into rabbit femurs for 4 weeks and 12 weeks, bone ingrowth into 400 μm scaffolds was significantly less than bone ingrowth into 600 and 800 μm scaffolds. Push-out tests also show that 400 μm scaffolds have inferior interfacial strength than the rest groups.

Conversely, pore sizes that are too large are not conducive to cell adhesion [125, 140]. Excessive pore size may be more like a macro plane than a 3D pore structure for cells. Moreover, cell seeding efficiency decreases as the pore size increases [126]. Many studies confirm that excessively large pores are not conducive to screw–bone bonding. Ran et al. [126] and Taniguchi et al. [127] showed that the 600 μm porous scaffolds bind bone more strongly than 800 and 900 μm porous scaffolds, respectively. The study of Hara et al. shows that the bone ingrowth into 1000 μm porous scaffolds is inferior to that into 500–800 μm porous scaffolds [133]. Fukuda et al. [141] implanted longitudinal square channels with pore sizes of 500, 600, 900, and 1200 μm into the dorsal muscles of beagle dogs to study osteoinduction and reported that the osteoinductive ability of 900 and 1200 μm pores is inferior to that of 500 and 600 μm pores. Overall, AM osseointegrated screws with 500–800 μm pore size may provide the best fixation.

TPMS design for additive-manufactured osseointegrated screws

TPMS-designed osseointegrated bone screws offer mechanical and biological advantages over conventionally designed porous screws. Most porous structures manufactured by AM are designed based on unit cells with polyhedral pores, straight edges, and sharp turns. TPMS, with zero mean curvature at all locations, can expand infinitely in the three-period directions [138]. TPMS exists in four common types: primitive surface (P surface), diamond surface (D surface), Gyroid surface (G surface), and I-wrapped package surface (IWP surface). These are expressed as follows [142, 143]:

$$P \text{ surface} : \cos X + \cos Y + \cos Z = c, \tag{3}$$

$$D \text{ surface} : \cos Z \sin(X + Y) + \sin Z \cos(X - Y) = c, \tag{4}$$

$$G \text{ surface} : \sin X \cos Y + \sin Y \cos Z + \cos X \sin Z = c, \tag{5}$$

$$IWP \text{ surface} : 2\left(\cos X \cos Y + \cos Y \cos Z + \cos Z \cos X\right) \\ - \left(\cos(2X) + \cos(2Y) + \cos(2Z)\right) = c, \tag{6}$$

where (X, Y, Z) represents the Cartesian coordinate system and c is the level-set constant, which results in significant variation in the local TPMS geometry.

According to the process of generating TPMS, TPMS can be divided into network TPMS and sheet TPMS. TPMS is a continuous non-self-intersecting surface that splits a space into two subspaces. Network TPMS fills a subspace with materials, whereas sheet TPMS uses materials to give the surface a certain thickness [144]. The advantage of network TPMS lies in better manufacturability and connectivity [145, 146]. During the AM process, it is easy to form a molten pool under the curved surface of sheet TPMS, resulting in powder adhesion and decreased porosity. However, sheet TPMS has superior mechanical properties and a higher surface-area-to-volume ratio, meaning larger bone tissue attachment area within a given volume [147]. The study by Al-Ketan et al. shows that sheet TPMS has better mechanical properties than network TPMS and a larger surface area for the same pore size and porosity [115]. The study of Cai et al. also shows that the compressive strength of sheet TPMS is 1.3 to 2 times that of network TPMS. The toughness produced by sheet TPMS also exceeds that of network TPMS [148]. Therefore, sheet TPMS may be more suitable for porous screws than network TPMS.

Mechanical advantages of TPMS-designed osseointegrated screws

TPMS-designed osseointegrated bone screws are mechanically superior compared with beam-based designs. At low porosity, the porous structure only weakly affects the mechanical properties of screws. In contrast, with increasing porosity, the porous structure more strongly affects the mechanical properties [115], and high porosity is beneficial for the osseointegration of screws. Compression tests demonstrate that the strength and toughness of sheet-TPMS scaffolds are superior to those of beam-based scaffolds

(Figs. 4d and 4e). Toughness is the area under the stress–strain curve at 25% strain and indicates the amount of energy required to damage the material [115]. A possible damage mechanism is that the structural design influences the deformation mode, with beam-based scaffolds mostly exhibiting mixed deformation modes, whereas sheet-TPMS structures are predominantly tensile [115]. Torsional tests show that the TPMS design may increase torsional strength and energy absorption capacity compared with beam-based designs. Torsional loading is a more complex condition than compression and tension loading because the direction of the load is constantly changing as the load is applied. Therefore, TPMS structures that are extended in all directions possess better torsional resistance (Fig. 4f) [149]. In addition, the excellent flexural resistance of TPMS structures has been verified by three-point bending tests and is widely used in sandwich structures [150, 151]. Bobbert et al. demonstrated through compression fatigue tests that the maximum endurance of TPMS scaffolds could reach 60% of the yield stress at a failure threshold of 1×10^6 cycles, which is at least threefold greater than the maximum endurance limit of beam-based scaffolds [138]. Compared with beam-based designs, TPMS design improves the fatigue performance of porous screws by reducing the stress concentration, which is the leading cause of fatigue failure [152, 153]. Therefore, TPMS-designed porous bone screws should have greater mechanical strength, which reduces the risk of screw breakage.

Biological advantages of TPMS-designed osseointegrated screws

TPMS-designed screws also have biological advantages. Bone remodeling is done layer by layer on the scaffold surface, so a larger surface area facilitates bone deposition [154, 155]. Al-Ketan et al. showed that the surface-area-to-volume ratio of TPMS can be twice that of beam-based scaffolds [115]. A higher surface-area-to-volume ratio means that TPMS provides more area for bone tissue attachment within the same volume.

More impressively, TPMS has the same mean curvature as bone trabeculae. The presence of surface stress related to curvature affects the reconstruction of bone tissue [156, 157]. In vitro experiments show that TPMS promotes the proliferation of osteoblasts and improves osteogenesis compared with beam-based structures [29, 158]. The results of lamin A/C (nuclear membrane protein) staining and immunofluorescence co-staining of F-actin and vinculin indicate that TPMS may induce the reorganization of the cytoskeleton of human mesenchymal stem cells and further impose external forces on the cell nucleus, thereby affecting its morphology. Such regulation of the nuclear morphology may lead to a cascade of cellular behavioral regulation, such as osteogenic differentiation and the promotion of angiogenesis (Fig. 4g)

[29]. Bone ingrowth was also significantly increased in the TPMS group compared with the beam-based cubic structure, suggesting that TPMS scaffolds with continuously curved surfaces can facilitate the infiltration of new tissue [29, 158].

The TPMS, especially the sheet-TPMS, has excellent mechanical properties and proven bone ingrowth capacity, which may be suitable for porous screws. Although TPMS-designed porous bone screws are currently available (FIREBIRD SI Fusion System, Orthofix, Texas, USA), the corresponding clinical cases to support them are lacking. In addition, dentistry researchers have considered designing root-simulating implants with TPMS as the basic unit [152]. In the future, TPMS-based porous screws should merit more in-depth research and validation.

Irregular trabecular-like design for additive-manufactured osseointegrated screws

Human trabecular bone is a random structure with no fixed shape, pore size, or local porosity (Fig. 5e). "Irregularity" is the term usually used to describe the degree of randomness. As the irregularity increases, the pore size distribution becomes broader and more uniform. Liang et al. [82] showed that about 90% of the pore size of the porous scaffold with a low irregularity of 0.06 is concentrated within 600–1000 µm. When the irregularity reaches 0.5, the pore size approaches the normal distribution within 100–2000 µm. Liang et al. also showed that bone cell proliferation and osteogenic ability are strongly related to the irregularity of the scaffolds [82]. Therefore, the irregular trabecular-like design may be another potential lever for improving the osseointegration of porous screws. The Voronoi-tessellation method has received increasing attention for constructing irregular bone tissue engineering scaffolds (Fig. 5e) [159]. A porous scaffold designed by the Voronoi method can exactly match the natural bone properties at all levels (microstructure, mechanical, mass transport, and biological properties) with optimum cell penetration, nutrient diffusion, and osteoconduction properties [30, 160].

Mechanical performance of bone trabecular-like designed osseointegrated screws

The mechanical properties are essential in trabecular-like designed osseointegrated screws. Huang et al. tested the bending and torsional resistance of trabecular-like designed screws with 55% porosity. The bending strength ((240.91 ± 108.00) N) and torque ((91.49 ± 12.08) N·cm) of trabecular-like designed screws are significantly less than those of solid screws (bending strength: (2056.52 ± 409.18) N; torque: (275.99 ± 127.39) N·cm) [78]. Like other types of porous structures, porosity is also a core parameter of the trabecular-like design and exerts an important influence
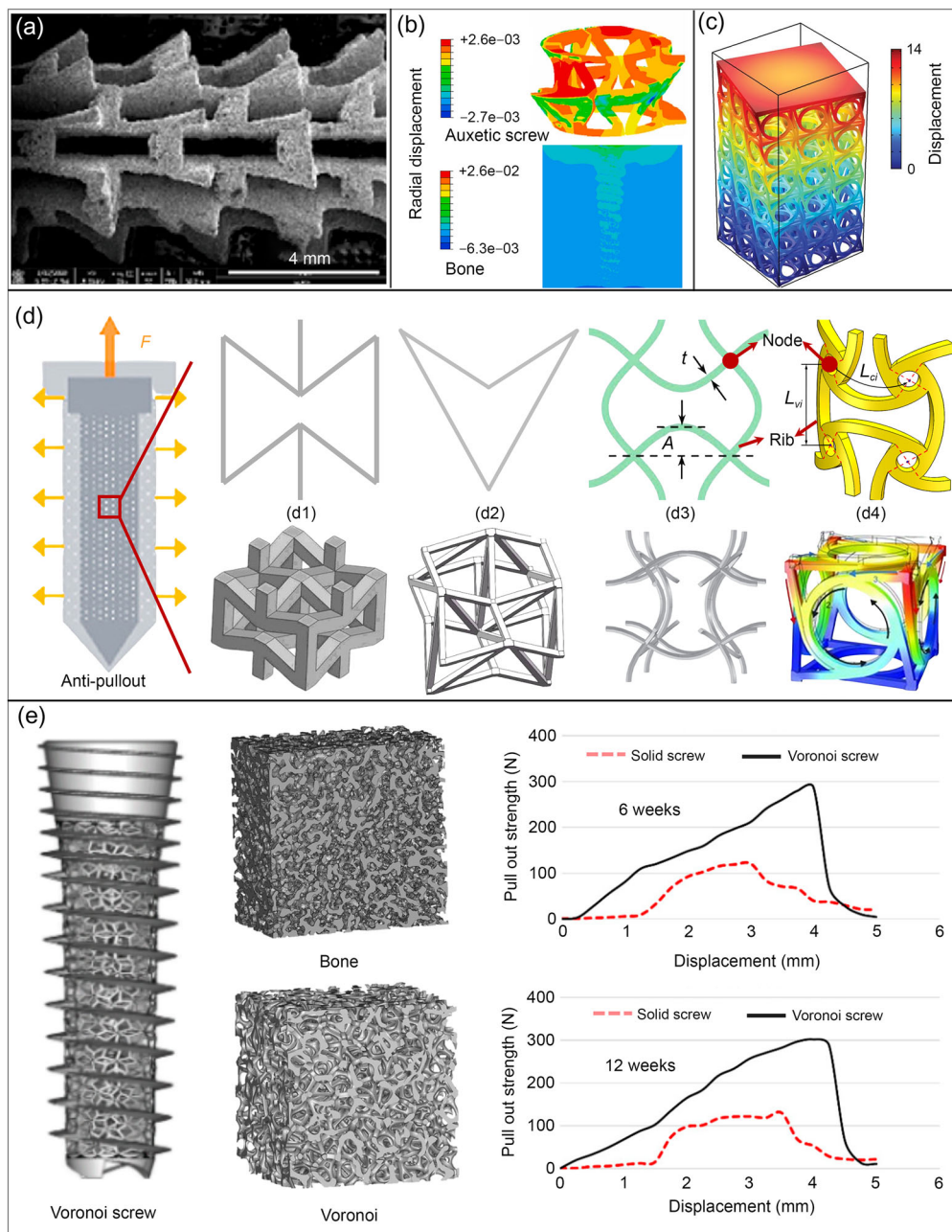
Fig. 5 Auxetic and irregular trabecular-like design for additive manufacturing (AM) osseointegrated screws. **a** Scanning electron microscopy (SEM) image of an auxetic-designed screw (reproduced from [172], Copyright 2021, with permission from Elsevier Ltd.). **b** Radial displacement of auxetic screw and bone under stretching (reproduced from [172], Copyright 2021, with permission from Elsevier Ltd.). **c** Radial shrinkage and torsional deformation of auxetic structure under compression (reproduced from [174], Copyright 2017, with permission from American Association for the Advancement of Science). **d** Schematic diagram of an auxetic screw and auxetic units of different structures: **d1** 2D and 3D (reproduced from [181], Copyright 2012, with permission from Acta Materialia Inc.) units of re-entrant hexagon structure; **d2** 2D and 3D (reproduced from [183], Copyright 2019, with permission from Elsevier Ltd.) units of double-V structure; **d3** 2D (reproduced from [180], Copyright 2021, with permission from Elsevier B.V.) and 3D (reproduced from [186], Copyright 2016, with permission from IOP Publishing Ltd.) units of sinusoidal ligaments; **d4** 2D (reproduced from [187], Copyright 2018, with permission from Elsevier Ltd.) and 3D (reproduced from [174], Copyright 2017, with permission from American Association for the Advancement of Science) units of the tetra-chiral structure. **e** Voronoi screw, Voronoi structure, and reconstructed 3D model of healthy trabecular bone (reproduced from [59], Copyright 2019, with permission from the authors, licensed under CC BY 4.0; reproduced from [82], Copyright 2019, with permission from Elsevier). Pull-out tests showed significantly higher pull-out strength for Voronoi screws at both 6 and 12 weeks

on its various properties. The apparent elastic modulus of the trabecular-like Ti_6Al_4V scaffolds with a porosity of 48.83%–74.28% after heat treatment is 1.93–5.24 GPa, and the ultimate yield strength is 44.9–237.5 MPa [82]. The trabecular-like Ti_6Al_4V scaffolds with irregularity (0.4) and porosity (70%, 80%, and 90%) after heat treatment have an elastic modulus range of 0.84–1.97 GPa and an ultimate strength range of 21.0–99.1 MPa [161]. The degree of irregularity also has an important influence on the mechanical properties of trabecular-like scaffolds. The apparent modulus of elasticity tends to decrease as the irregularity increases. However, the compressive strength fluctuates as a function of the irregularity. A slight degree of irregularity often decreases the strength caused by the initial instability of the unit on which the structure is based. When the irregularity exceeds a certain value, the structure forms a new stress balance, and the compressive strength tends to stabilize [162]. Chang et al. [59] showed that the mechanical properties of trabecular-like designed screws could be somewhat improved by optimizing the porous design.

Biological advantages of bone trabecular-like designed osseointegrated screws

The potential biological advantage is the main attraction of the bone trabecular-like design of porous bone screws. As described in "Effect of pore size and porosity on biological properties of additive-manufactured osseointegrated screws" section, large pores facilitate substance penetration, whereas small pores facilitate cell adhesion. The trabecular-like design with widely distributed pore size can simultaneously provide good permeability and high cell adhesion efficiency. Compared with conventional scaffolds (the octet, body-centered cubic, and pillar body-centered cubic), irregular scaffolds have a more uniform stress distribution and wider permeability [163]. A recent study has shown that scaffolds with different pore diameters could give cells more diverse stimulation, which is conducive to cell growth [164]. The studies by Cheng et al. [135] and Liang et al. [82] show that irregular scaffolds have better proliferation and osteogenic ability, which may be related to the up-regulation of the related gene expression. Wang et al. showed that irregular scaffolds have a greater vascularization capacity than regular porous scaffolds [165]. In vivo experiments also confirmed the excellent osseointegration ability of the structure. Ragone et al. [166] implanted a randomized trabecular titanium structure into sheep and proved that the structure underwent rapid osseointegration both in cancellous and cortical bone. Pull-out tests showed that the immediate stability of screws with a trabecular-like design did not differ from that of regular porous screws or solid commercial screws. However, after 6- and 12-week implantation, screws with a trabecular-like design exhibited the best stiffness and pull-out strength [59].

At the same time, this study indicates that irregular screws are more conducive to early osteogenesis, which is essential for the rapid recovery of patients.

The long-term fixation of trabecular-like porous bone screws (Zimmer Dental Inc., California, USA) has been extensively demonstrated in dentistry [35]. However, Zimmer screws are fabricated by chemical vapor deposition. The Voronoi-tessellation method combined with AM technology offers more design and manufacturing freedom, which can greatly expand the application scenario of trabecular-like designed porous screws.

Auxetic design for additive-manufactured osseointegrated screws

Auxetic structures have negative Poisson ratios (NPRs), expanding in tension and contracting in compression. All screws designed with the above-mentioned porous structure have a positive Poisson ratio, tending to contract in the transverse direction under lengthwise stretching. In contrast, auxetic porous screws with an NPR expand under stretching to enhance the fixation of screws to bone (Fig. 5b) [31].

Auxetic structures can be divided into re-entrant, chiral, rotating rigid (or semi-rigid), and other structures according to their deformation mechanism [167]. Classic examples of re-entrant structures are re-entrant hexagonal and double-V or double-arrow structures, whose main deformation mechanism is bending of the oblique strut [168–170]. Chiral units consist of central cylinders (nodes) connected by tangential elastic ligaments (ribs), whose deformation mechanisms consist of rotation of the nodes and bending of the ribs [167]. The auxiliary response of the rotating rigid structure is caused by the rotation of the rigid geometry around the hinge during tension [171]. Yao et al. [31] compared the mechanical properties of three types of auxetic screws and showed that the different auxetic structures change the mechanical properties of the screws, especially their functional properties. In particular, the re-entrant structures have the highest tensile strength and an NRP of greater magnitude.

According to the space form, auxetic structures can be divided into two-dimensional (2D) and 3D (Fig. 5d), determining their scope of application. It is obvious that 2D auxiliary structures cannot be applied to screws, and hollow screws can only be designed by transforming 2D auxiliary structures into 3D tubular structures (Fig. 5a) [172]. Another type of 3D auxetic structure comprises 3D auxetic cell arrays in three directions, X, Y, and Z. Kolken et al. [173] applied the 3D auxetic structure to the hip stem design to optimize stress transfer. Theoretically, 3D auxetic structures can also be applied to porous bone screws, which is a promising approach.

Mechanical advantages of auxetic-designed osseointegrated screws

The core advantage of auxetic screws is their unique mechanical deformation behavior—the screws expand radially under tension to resist pullout and improve screw fixation [172]. Frenzel et al. [174] reported a 3D tetra-chiral structure that undergoes torsional deformation in addition to radial shrinkage when compressed (Fig. 5c). Porous screws using this lattice might be easier to screw in because they twist and contract under compression and resist pullout by expanding under axial stretching.

In addition, auxetic porous materials have a higher shear strength than common porous materials [175]. For isotropic materials, the shear modulus G correlates positively to the elastic modulus E and negatively to the Poisson ratio v, as expressed by [171, 176]

$$G = \frac{E}{2(1+v)}. \tag{7}$$

Thus, auxetic screws are expected to offer high shear strength while maintaining a low elastic modulus. Another advantage of the auxetic structure is improved bending resistance, almost twice that of conventional materials, because material expansion tends to suppress crack propagation [176–178]. Jiang et al. [179] reported a tubular auxetic structure based on sinusoidal ligaments, with Poisson ratios ranging from −0.7 to 0. Three-point bending tests showed an 85.4% improvement in ductility compared with the diamond structure [180]. Compression tests showed that the compressive strength of porous scaffolds with comparable porosity increases significantly as the Poisson ratio decreases [176, 181]. In other words, the auxetic structure can deliver a relatively high compressive strength while maintaining high porosity. In addition, the auxetic structure has excellent energy absorption and impact resistance and is used in jounce bumpers [175, 182].

Furthermore, the mechanical properties of auxetic screws can be further optimized by improving the design. Yao et al. [31] found that increasing the wall thickness does not affect the Poisson ratio of the screws but could improve the tensile stiffness, strength, and breaking elongation rate. Further research confirmed that adjusting the re-entrant hexagon angle could change the Poisson ratio of auxetic pedicle screws [172]. By smoothing the corners, stress concentrations can be reduced while maintaining an NPR, further improving mechanical strength [183]. Based on the double-V structure, Guo et al. [184] developed the double-U design, whose smooth geometry configurations can reduce stress concentration in the elastic region and enhance the auxetic behavior during large deformation. Meena and Singamneni [185] designed a novel S-shaped structure with less stress concentration than re-entrant structures and with no cracking or failure of the elements of the structure.

In summary, auxetic screws have excellent mechanical properties and an NPR, which enhances fixation.

Biological performance of auxetic-designed osseointegrated screws

The tensile-expansion-deformation behavior of auxetic screws also gives them a biological advantage, especially in ligament reconstruction. Early stabilization of the bone–screw interface and adequate stress stimulation are essential for robust screw–bone integration. Excessive micromotion during the early stages of screw implantation may lead to the formation of fibrous tissue around the screw rather than bone formation [56]. In addition, according to Wolff's law, bone resorption typically occurs if the bone surrounding the screw does not receive sufficient stress stimulation [132, 188]. However, in ligament reconstruction, the ligament tends to exert tension on the screws, which leads to excessive micromovement of the screw in the bone tunnel [189]. Tensile loads also shrink porous screws with positive Poisson ratios [31]. Therefore, widening of the bone tunnel around a screw is often reported in ACLR, implying that the screw fails to integrate well with the bone [52, 53]. Interestingly, auxetic screws could resist pullout by radial expansion when subjected to a tensile force [31]. This increased stability should provide an interface that facilitates screw–bone integration. Conversely, radial expansion means that auxetic screws convert axial tension into radial pressure, which facilitates better mechanical stimulation of the bone [31, 172]. Finite-element analysis (FEA) showed that under a tension of 250 N, the auxetic screws expanded radially by 1.5 μm, while the nonauxetic screws underwent a radial shrinkage of 1.0 μm [190]. In vitro experiments showed that auxetic scaffolds effectively deliver biomechanical stimuli and promote periodontal ligament cell proliferation and osteogenic capacity [191]. In addition, adequate mechanical loading inhibits the expression of osteoclasts, retarding the resorption of peri-implant bone tissue [192]. Wang et al. [190] implanted auxetic screws in a rabbit femur and subjected them to cyclic tensile loads. The results showed that the osseointegration parameters of the auxetic screw, such as bone volume fraction, number of trabeculae, and trabecular thickness, improved more than those of nonauxetic screws after six-week implantation under in vivo dynamic tensile loading. These studies suggested that auxetic screws offer unique biological advantages in ligament reconstruction and should provide a reliable anchor for ligaments through stronger screw–bone integration.

In summary, the tensile-expansion-deformation behavior of auxetic screws translates into more efficient load

transmission and improves stabilization, which favors screw–bone integration, especially under tensile loading.

Macro design of additive-manufactured osseointegrated screws

Porous screws can achieve bone ingrowth, thereby improving long-term fixation. However, as described in "Effect of pore size and porosity on mechanical properties of additive-manufactured osseointegrated screws" section, porosity dramatically reduces the mechanical properties of these screws and increases the risk of screw fracture. By optimizing the overall distribution of the material through macro design, porous screws can provide sufficient mechanical strength while preserving pores for bone ingrowth. Graded design, gradient design, and topology optimization design are three strategies that optimize material distribution.

Gradient design and graded design for additive-manufactured osseointegrated screws

Gradient and graded designs are similar strategies for designing porous screws, with the relatively dense portion providing mechanical strength and the relatively porous portion providing space for bone ingrowth. Gradient design refers to a change of porosity along a specific direction, manifested as a gradual change in the mechanical and biological properties [193]. At the same time, gradient design has no transition zone between different parts [26]. These two strategies are reasonable solutions to the contradiction between improving biological properties and reducing mechanical properties. Davoodi et al. [128] designed a porous gradient implant with a porosity ranging from 0.25 to 0.75, linearly varying from the center to the surface. Compared with a uniform design with similar porosity, this gradient design increases the longitudinal permeability of the implant by 60% without losing its transverse permeability. At the same time, compression tests showed that compared with a uniform porosity distribution, the gradient distribution of porosity improves the overall mechanical performance of the scaffold. Torsional tests showed that gradient design increases torsional stiffness by 35% and ultimate shear strength by 15% compared to the uniform design [194].

The graded design can also enhance the mechanical properties of the porous screw. Zhang et al. [195] showed that for a given porosity, the graded scaffold has a similar elastic modulus as the uniform scaffold yet a higher yield strength. FEA showed that the denser part carries larger stresses, significantly improving the scaffold's overall strength. The compressive strength of the graded-porosity scaffold is nearly 46% greater than that of the uniform-porosity scaffold when the overall porosity is approximately

the same [196]. In addition, the graded design improves the fatigue performance compared with uniform design [197]. Xiong et al. [26] designed a porous graded bone screw with a dense core (Fig. 6) and, by adjusting the diameter of the dense core, improved the static mechanical and fatigue properties of the screw.

To summarize, by ensuring space for bone ingrowth, the gradient design and graded design improve the mechanical properties of screws and reduce the chance of breakage.

Topology optimization design for additive-manufactured osseointegrated screws

Topology optimization is a method of systematically optimizing the distribution of implant materials to optimize the load-transmission mechanism [33]. The development of digital technology allowed topology optimization to be combined with FEA. The stiffness requirements of different parts of the implants can be obtained by FEA [198]. Topological optimization increases the distribution of the material in stress concentration areas to avoid implant failure. For instance, Zhang et al. [33] designed a new proximal tibial prosthesis by topology optimization, significantly optimizing its biomechanical and biological properties. Due to the richness of screw application scenarios, some screws also concentrate stress. The FEA results of Song et al. [199] showed that the stress distribution of screws in lumbar fusion is not uniform and concentrates mainly at the screw root. The screws used to treat femoral neck fractures also suffer from stress concentration [200]. Based on the deterioration of the mechanical properties caused by screw porosity, stress concentration significantly increases the risk of screw breakage. Topology optimization technology increases the strength of the stress concentration area of screws, thereby reducing the risk of screw breakage. Some researchers improved the rod in spinal fixators through topology optimization to reduce stress concentration in pedicle screws [32, 201]. However, the topology optimization for a screw itself has not yet been studied. According to the FEA results, increasing the material distribution in the stress concentration region of the screw is vital and needs to be developed in future studies.

To summarize, the mechanical performance of AM porous screws can be improved by macro design, including gradient design, graded design, and topology optimization. However, optimizing the design cannot decrease the loss in the mechanical strength of screws caused by AM defects.

Process and material improvement of additive-manufactured osseointegrated screws

AM offers unprecedented advantages over traditional techniques of manufacturing porous bone screws. Traditional
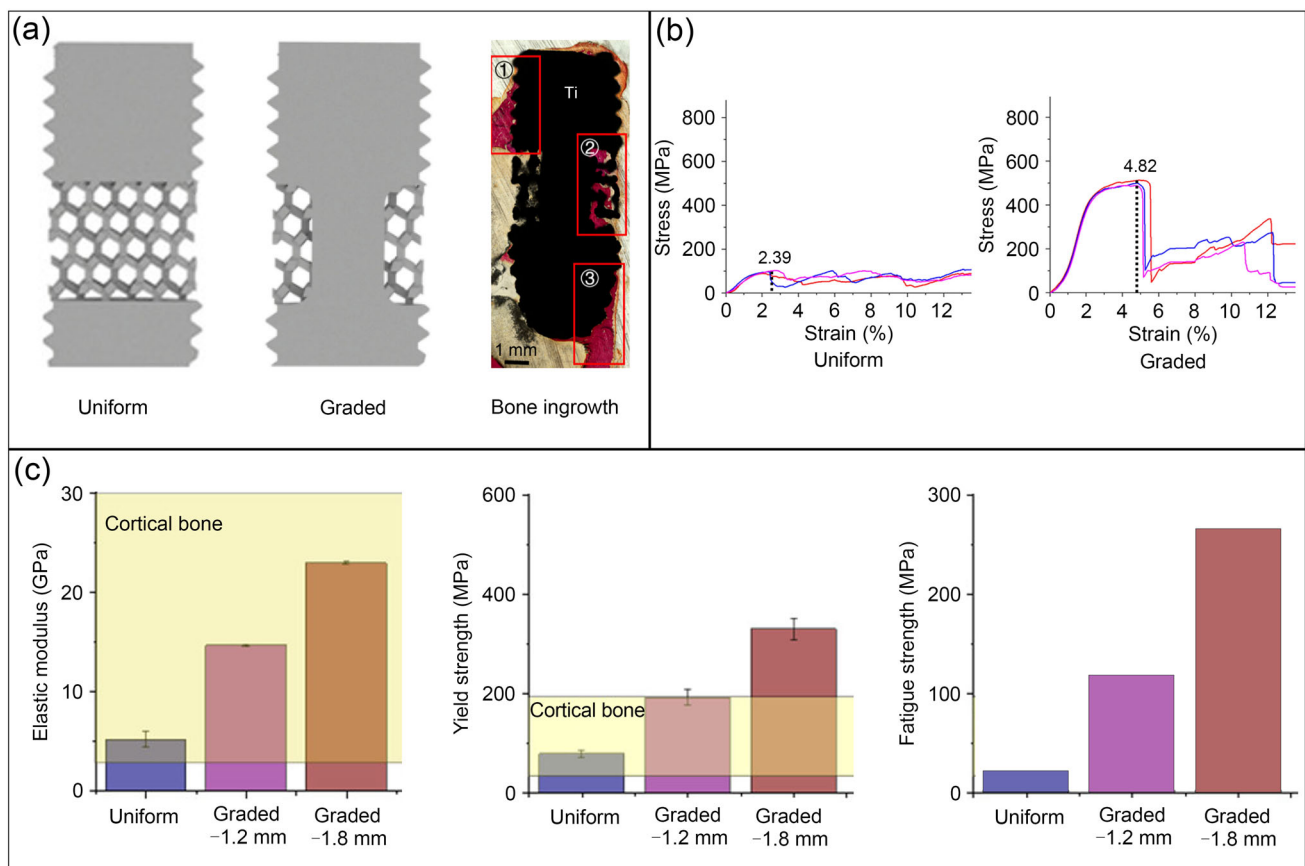
Fig. 6 Graded design for additive manufacturing (AM) osseointegrated screws (reproduced from [26], Copyright 2020, with permission from the authors, licensed under CC BY 4.0). **a** Schematic diagram of uniform porous screw and graded screw and histological image of graded screw. **b** Stress–strain curves of uniform porous screw and graded screw. **c** Elastic modulus, yield strength, and fatigue strength of uniform porous screw and graded screw

screws are made through cutting, which can be done by turning, milling, or grinding. The initial material from which a screw is made is called "bar stock," which usually is a cylindrical rod with a diameter approximating the largest diameter of the screw [34]. After turning, the bar is transformed into screws of specific sizes. Although traditional screw manufacturing methods have the advantages of large batches, low cost, and high efficiency, using these methods to manufacture porous screws is challenging. Basically, efficiently producing screws with complex designs is impossible with traditional methods. AM can be used to manufacture porous screws of the aforementioned design through a layer-by-layer manufacturing process (Fig. 7a) [26, 59, 78, 172]. However, AM porous screws have the problem of discrepancies between as-built products and predesigned models, which can decrease their mechanical strength.

First, the layer-by-layer AM process and residual stresses may lead to delamination between layers and deformation in AM screws [161, 202]. Second, in the manufacturing process of porous screws, internal voids and cracks form inside the

solid part of the porous structures (Fig. 7c) [203]. The ideal AM porous screw should be porous, but the inside of the solid struts that make up the pores should be dense. However, internal void defects appear within the struts of porous scaffolds fabricated by powder bed fusion (PBF) [122, 202]. These small voids or cracks decrease the fatigue strength [39]. The reduction in porosity is another discrepancy between as-built products and predesigned models, which is common in AM based on PBF due to partially adhered powders on the surface of the scaffolds [40]. This phenomenon is caused by the thermal diffusion of loose powders and solidified material, partial melting of boundary metal powders by the contour laser track, and building the curved struts of porous parts on the loose powders, resulting in the formation of a small melt pool [122, 204]. These partially adhered powders may act as crack-initiation sites at the surface, further shortening the fatigue life [118]. Manufacturing defects and residual stress play an important role in crack initiation and propagation [86, 161], which may fracture AM porous screws after implantation. In addition, with PBF technology, the rapid cooling
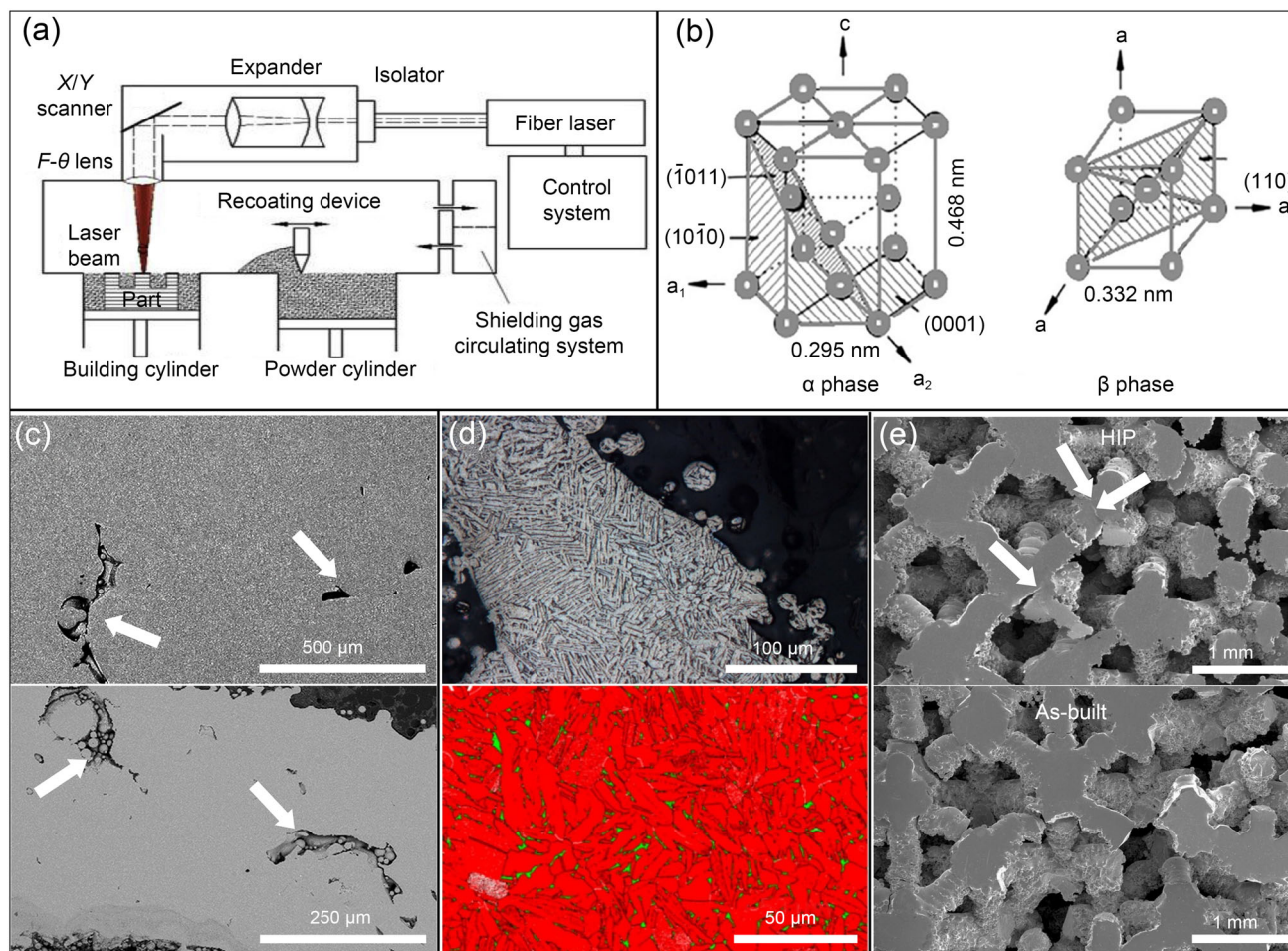
Fig. 7 Schematic diagram, defects, and post-treatment of additive manufacturing (AM) screws. **a** Schematic diagram of a selective laser melting (SLM) machine (reproduced from [237], Copyright 2015, with permission from Elsevier Ltd.) **b** α and β phases of titanium (reproduced from [212], Copyright 2012, with permission from Acta Materialia Inc.). **c** Internal voids in the strut (reproduced from [204], Copyright 2017, with permission from Elsevier Ltd.). **d** Optical microscopy image and β-phase distribution map of the hot isostatic pressing (HIP) sample, where green represents β-Ti and red represents α-Ti (reproduced from [86], Copyright 2018, with permission from Acta Materialia Inc.). **e** Fatigue cracks are blunt passivated in HIP samples but not as-built samples (reproduced from [41], Copyright 2017, with permission from Elsevier Ltd.)

after heating causes screws made of Ti_6Al_4V to enter a relatively brittle acicular martensite α phase, which reduces the fatigue life of the screws [86]. Therefore, we must improve the manufacturing of AM screws to enhance their mechanical properties.

Process improvement of additive-manufactured osseointegrated screws

Research advances throughout the AM process reduce defects in AM screws and improve the mechanical strength. Preheating the powder before printing reduces the residual stress, internal porosity, and cracking [205, 206]. Ali et al. significantly reduced residual stresses in the printed product by preheating the powder bed to 570 °C, resulting in a 3.2% and 66.2% increase in yield strength and elongation of the manufactured product, respectively [206]. Polozov et al. found that preheating above 600 °C produces products without internal cracks, and the highest tensile strength was manufactured at a preheating temperature of 980 °C [207]. During manufacturing, defects can also be reduced by optimizing the process parameters. For example, reducing the layer thickness improves manufacturing accuracy, which is often better in SLM than in electron-beam melting due to the smaller layer thickness in SLM [81, 172]. In addition, for SLM, the volumetric energy density $E_{density}$ is a composite indicator of the response energy input. The energy density can be expressed as [208]

$$E_{density} = \frac{P_{laser}}{sht},$$

(8)

Table 3 β-phase fraction and internal porosity of different heat treatment methods (reproduced from [86], Copyright 2018, with permission from Acta Materialia Inc.)

Group type	β phase (%; mass fraction)	Internal porosity (%; area fraction)
As manufactured	0	1.2±0.6
Annealed at 800 °C for 150 min	9.6±0.6	1.3±0.7
HIP	11.5±1.5	0.1±0.1
Annealed at 1050 °C for 150 min	20.4±0.5	1.4±0.6

HIP: hot isostatic pressing

where P_{laser} is the laser power, s is the scanning speed, h is the hatch distance, and t is the layer thickness. The proper energy input plays a vital role in the densification of SLM products, which requires a combination of high laser power and high scanning speed or low laser power and low scanning speed [208].

Heat treatment remains the only option to improve the mechanical properties of as-manufactured screws [209]. Stress-relief annealing can remove residual stress and avoid premature deformation and fracture of porous structures due to stress concentration in fatigue tests. The number of cycles for the scaffolds increases by at least 80% after stress-relief annealing [161]. The study by Liang et al. also showed that the specimens had a greater ultimate strength after stress-relief annealing (600 °C, furnace cooling) because it avoids premature deformation and fracture by relieving residual stress [82]. This study also showed that fully annealed (840 °C, furnace cooling) specimens had higher yield plasticity. After full annealing, the inhomogeneous martensite structure transforms into a stable coarse-grained structure and, finally, a basket structure. Fatigue tests showed that scaffolds with the same porosity could cycle over four times more than unannealed scaffolds after full annealing [161]. Furthermore, hot isostatic pressing (HIP) treatment substantially reduces the internal porosity of the scaffold matrix and transforms the microstructure into a more ductile mixture of α+β phases (Fig. 7d) (Table 3) [41, 86]. The presence of the β phase provides more ductility to AM porous screws. The tougher α+β phase blunts the fatigue cracks and improves the fatigue performance compared with the brittle α phase. Figure 7e shows that fatigue cracks are blunted in the HIP scaffolds, whereas no crack blunting occurs in the SLM specimens [41]. The fatigue-endurance ratio of the SLM lattice after HIP treatment at 1×10^{6} cycles reaches a level equivalent to that of solid metals [210]. Wu et al. showed that, at 1000 °C and 150 MPa, HIP treatment eliminates the voids in

the struts, reduces the microhardness from 403 to 324 HV, reduces the yield strength from 143 to 100 MPa, and increases the fatigue-endurance ratio from 0.3 to 0.55, which is comparable to the fatigue-life ratio of solid metal materials [41].

Material improvement of additive-manufactured osseointegrated screws

In addition to optimizing the manufacturing process of AM screws, optimizing the screw material can improve their performance. Early screws were mainly made of stainless steel, but their biocompatibility was poor, so titanium alloys gradually replaced them.

However, the elastic modulus of titanium alloys is much greater than that of bones. At the same time, the screws require sufficient mechanical strength to avoid breakage. The development of β-titanium alloys offers a potential solution to this paradox. The introduction of the β phase in titanium alloys depends mainly on alloying elements and thermomechanical processes [211]. At room temperature, titanium is characterized by a hexagonal close-packed crystal structure known as the α phase. When heated above 882 °C, the structure transforms into a body-centered cubic structure called the β phase (Fig. 7b) [86]. Some alloying elements, such as Al, C, and O, increase the transition temperature; these are called α stabilizing elements. Other alloying elements, such as Ta, V, Fe, and Nb, reduce the transformation temperature and are called β stabilizing elements [212]. In addition, the cooling process of the β phase affects the final microstructure of titanium alloys, producing the α′ or α″ phase [42]. The advantage of β-titanium alloy lies in its low elastic modulus and relatively high strength-to-modulus ratio [42]. Low elastic modulus means better avoidance of stress-shielding phenomenon, even with lower porosity. A higher strength-to-modulus ratio indicates that the screws have higher mechanical strength under the same elastic modulus. The elastic modulus of β-type Ti–24Nb–4Zr–8Sn with 75% porosity is only 0.95 GPa, while the strength can reach 50 MPa [213]. Although no β-titanium alloy screws have yet been reported in the literature, these porous β-titanium alloys fabricated by PBF have demonstrated their feasibility [211, 213]. When the elastic modulus of Ti_6Al_4V is reduced to 1.3 GPa, the strength is only 18.8 MPa [38]. Table 4 summarizes the mechanical properties of inert metals that can be used in screw fabrication. The development of β-titanium alloy should produce a new type of screw with low elastic modulus and high mechanical strength.

Titanium alloys have good in-body stability and corrosion resistance and are widely used for screws that need to provide long-term retention. However, in some orthopedic diseases, such as fractures and hallux valgus, screws only serve for temporary fixation. Once the bone heals, the screw

Table 4 Elastic modulus and strength of various types of titanium alloys

Composition	Type	Elastic modulus (GPa)	Strength (MPa)	References
Pure Ti	α	105	170–485	[214]
Ti_6Al_4V	$\alpha+\beta$	114	825–869	
Ti_6Al_7Nb	$\alpha+\beta$	110	800–1000	[215]
$Ti_{15}Ta_5Zr$	β	42.2	445.7	[216]
$Ti_{20}Nb_{10}Zr_5Ta$	β	59	566	[217]
$Ti_{30}Nb_5Ta_3Zr$	β	64.2	680	[218]
$Ti_{21}S$	β	52 ± 0.3	709 ± 6	[219]
$Ti_{25}Ta$	α''	64	480	[214]
$Ti_{15}Nb_9Zr$	α'	39	850	[42]

is no longer necessary [220, 221]. Thus, the upside (osseointegration) can also be the downside (difficult to remove) if removal is required. Absorbable screws do not require secondary-surgery removal, which avoids the pain and costs of secondary surgery for patients. A variety of absorbable materials can be used to manufacture AM screws. Most absorbable screws currently used clinically are polylactic acid materials [25, 51]. However, screws made of these biodegradable synthetic polymers often face problems such as fractures due to insufficient mechanical strength [222]. Biodegradable metallic screws (Fe, Zn, and Mg) may be a good choice because they combine high mechanical strength with gradual degradation [223–225]. According to the metal activity order, the metals' degradation rates may be ranked as follows: Mg>Zn>Fe. Iron-based screws have excellent mechanical properties and the slowest degradation. Tai et al. [226] and Liu et al. [224] fabricated biodegradable Fe-based porous screws by SLM. The biosafety of Fe-based screws was verified in the rabbit rotator-cuff tear model and rabbit lateral femoral condyle model [224, 226]. However, further clinical application of iron-based screws remains challenging due to the magnetic properties of Fe and the production of iron-oxide degradation by-products [227]. The slow degradation rate of Fe-based screws is also a drawback [226]. The degradation rate of Zn lies between that of Fe and Mg. Recently, Zn-based degradable orthopedic implants have received increasing attention due to their osseointegration-promoting effect and mechanical strength (close to that of pure titanium) [228]. Montani et al. [229] explored the feasibility of preparing Zn-based implant materials by PBF. Subsequently, Wen et al. [230] applied a porous Zn scaffold prepared by SLM to biomedicine. Qu et al. [225] reported Zn_2Ag-based screws with both osseointegration-promoting and antibacterial effects. Zinc-based screws have great potential as a new type of orthopedic screw and merit further in-depth exploration. Of the three metals, Mg-based screws are the most studied and have achieved good results in clinical practice [221]. Different Mg-based screws, including MgYREZr screws [220, 231], high-purity Mg screws [232],

and Mg–Zn–Ca screws [233], have been validated in clinical trials in different countries. Although good clinical results have been achieved, the rapid degradation rate and relatively poor mechanical strength of magnesium-based screws remain challenging to solve [231, 234]. Magnesium alloys are also challenging for AM due to the high chemical reactivity, which poses a risk of combustion [235]. To solve these problems, some researchers have tried to develop Mg-Ti hybrid screws composed of Mg rod and Ti-based interference screws with holes in the screw body [223, 234]. Encouragingly, Li et al. [236] fabricated porous Mg-based scaffolds using SLM, laying the foundation for AM Mg-based screws. In conclusion, for screws that need to be removed surgically, degradable screws have excellent development prospects. Material advances will have a profound and epoch-making impact on the development of screws.

To summarize, AM offers unique advantages for manufacturing porous screws. Although the current AM screws have certain defects, the advancement of AM and materials should endow AM screws with greater mechanical strength.

Summary and challenges

Screw fixation has always been widely used in clinical practice. With the development of medical technology, especially the emergence of permanent orthopedic implants such as various prostheses, the long-term fixation capacity of screws has become an urgent problem to solve. In earlier research, screw optimization mainly focused on the profile design to improve the initial stability. However, conventional, smooth solid screws have poor osseointegration and suffer from long-term loosening. AM technology produces porous screws, which are expected to have a suitable elastic modulus to avoid stress shielding while allowing bone ingrowth. Macro designs and the improvement of AM can balance the reduction in mechanical strength of screws caused by porosity and AM defects. Furthermore, surface modification can improve the osseointegration capacity of porous screws and achieve a stronger

bone–screw combination. AM osseointegrated screws with hierarchical design can act as "roots" in the bone to further fix various prostheses or for joint fusion. In the future, the continuous optimization of the osseointegration screw will further expand the scope of its clinical applications.

Note that AM osseointegrated screws with hierarchical design also face some challenges:

1. More comprehensive experimental validation is needed for the fixation effect of AM bone screws: including in vitro and in vivo pull-out tests at different stages of implantation to validate the immediate and long-term fixation of AM screws.
2. The mechanical properties of AM bone screws are inferior to those of conventional solid screws. Therefore, more comprehensive mechanical testing of AM bone screws, including torsion test, three-point bending test, tensile test, compression test, and fatigue test, is needed to ensure their mechanical safety. However, a comprehensive and unified mechanical property test standard for AM bone screws is currently lacking. The development and unification of relevant standards will greatly facilitate the development of AM bone screws.
3. AM screws still have many manufacturing defects that may weaken their mechanical properties. Recent advances in AM technology may help improve the mechanical strength of screws
4. For screws destined for temporary fixation and requiring removal by secondary surgery, absorbable screws are worthy of in-depth study.
5. The biosafety, clinical ethics, and pre-implantation sterilization procedures of surface-modified screws must be confirmed, especially as concerns surface modification with bioactive factors.

Declarations

Conflict of interest The authors declare that they have no conflict of interest.

Ethical approval This article does not contain any studies with human or animal subjects performed by any of the authors.

References

1. Vuletic M, Pelivan I, Gabric D (2021) Implant prosthodontic rehabilitation after surgical treatment for an oropharyngeal malignant tumour using tantalum dental implants. Case Rep Dent 2021:5585181. https://doi.org/10.1155/2021/5585181
2. Upfill-Brown A, Satariano N, Feeley B (2019) Stemless shoulder arthroplasty: review of short and medium-term results. JSES Open Access 3(3):154–161. https://doi.org/10.1016/j.jses.2019.07.008
3. Kranenburg A, Garcia-Diaz G, Cook JH et al (2022) Revision of failed sacroiliac joint posterior interpositional structural allograft stabilization with lateral porous titanium implants: a multicenter case series. Med Devices (Auckl) 15:229–239. https://doi.org/10.2147/MDER.S369808
4. Jain S, Eltorai AEM, Ruttiman R et al (2016) Advances in spinal interbody cages. Orthop Surg 8(3):278–284. https://doi.org/10.1111/os.12264
5. Moroni A, Faldini C, Pegreffi F et al (2004) HA-coated screws decrease the incidence of fixation failure in osteoporotic trochanteric fractures. Clin Orthop Relat Res 425:87–92. https://doi.org/10.1097/01.blo.0000132405.30139.bb
6. Mudgal CS, Jupiter JB (2006) Plate and screw design in fractures of the hand and wrist. Clin Orthop Relat Res 445:68–80. https://doi.org/10.1097/01.blo.0000205887.04200.21
7. Shea TM, Laun J, Gonzalez-Blohm SA et al (2014) Designs and techniques that improve the pullout strength of pedicle screws in osteoporotic vertebrae: current status. Biomed Res Int 2014:748393. https://doi.org/10.1155/2014/748393
8. Wang T, Boone C, Behn AW et al (2016) Cancellous screws are biomechanically superior to cortical screws in metaphyseal bone. Orthopedics 39(5):E828–E832. https://doi.org/10.3928/01477447-20160509-01
9. Phan K, Hogan J, Maharaj M et al (2015) Cortical bone trajectory for lumbar pedicle screw placement: a review of published reports. Orthop Surg 7(3):213–221. https://doi.org/10.1111/os.12185
10. DeCoster TA, Heetderks DB, Downey DJ et al (1990) Optimizing bone screw pullout force. J Orthop Trauma 4(2):169–174. https://doi.org/10.1097/00005131-199004020-00012
11. Finlay JB, Harada I, Bourne RB et al (1989) Analysis of the pull-out strength of screws and pegs used to secure tibial components following total knee arthroplasty. Clin Orthop Relat Res 247(247):220–231. https://doi.org/10.1097/00003086-198910000-00032
12. Santos ER, Sembrano JN, Mueller B et al (2011) Optimizing iliac screw fixation: a biomechanical study on screw length, trajectory, and diameter. J Neurosurg Spine 14(2):219–225. https://doi.org/10.3171/2010.9.SPINE10254
13. Adell R, Lekholm U, Rockler B et al (1981) A 15-year study of osseointegrated implants in the treatment of the edentulous jaw. Int J Oral Surg 10(6):387–416. https://doi.org/10.1016/s0300-9785(81)80077-4
14. Brånemark PI, Hansson BO, Adell R et al (1977) Osseointegrated implants in the treatment of the edentulous jaw: experience from a 10-year period. Scand J Plast Reconstr Surg Suppl 16(10):1–132

15. Albrektsson T, Branemark PI, Hansson HA et al (1981) Osseointegrated titanium implants: requirements for ensuring a long-lasting, direct bone-to-implant anchorage in man. Acta Orthop Scand 52(2):155–170. https://doi.org/10.3109/17453678 108991776

16. Bencharit S, Byrd WC, Altarawneh S et al (2014) Development and applications of porous tantalum trabecular metal-enhanced titanium dental implants. Clin Implant Dent Relat Res 16(6):817–826. https://doi.org/10.1111/cid.12059

17. Das K, Bose S, Bandyopadhyay A (2009) TiO$_2$ nanotubes on Ti: influence of nanoscale morphology on bone cell-materials interaction. J Biomed Mater Res A 90A(1):225–237. https://doi.org/10.1002/jbm.a.32088

18. Ren B, Wan Y, Liu C et al (2021) Improved osseointegration of 3D printed Ti-6Al-4V implant with a hierarchical micro/nano surface topography: an in vitro and in vivo study. Mater Sci Eng C 118:111505. https://doi.org/10.1016/j.msec.2020.111505

19. Kloss FR, Singh S, Haechl O et al (2013) BMP-2 immobilized on nanocrystalline diamond-coated titanium screws; demonstration of osteoinductive properties in irradiated bone. Head Neck 35(2):235–241. https://doi.org/10.1002/hed.22958

20. Zhao XY, Cao X (2023) Dual-functional coating that inhibits bone resorption and promotes bone formation applied to the surface modification of titanium screws. Mater Lett 349:134734. https://doi.org/10.1016/j.matlet.2023.134734

21. Nemcakova I, Litvinec A, Mandys V et al (2022) Coating Ti6Al4V implants with nanocrystalline diamond functionalized with BMP-7 promotes extracellular matrix mineralization in vitro and faster osseointegration in vivo. Sci Rep 12(1):5264. https://doi.org/10.1038/s41598-022-09183-z

22. Li S, Yuan HF, Pan JF et al (2017) The treatment of femoral neck fracture using VEGF-loaded nanographene coated internal fixation screws. PLoS ONE 12(11):e0187447. https://doi.org/10.1371/journal.pone.0187447

23. Li Y, Fellander-Tsai L (2021) The bone anchored prostheses for amputees: historical development, current status, and future aspects. Biomaterials 273:120836. https://doi.org/10.1016/j.biomaterials.2021.120836

24. Pobloth AM, Checa S, Razi H et al (2018) Mechanobiologically optimized 3D titanium-mesh scaffolds enhance bone regeneration in critical segmental defects in sheep. Sci Transl Med 10(423):eaam8828. https://doi.org/10.1126/scitranslmed.aam8828

25. Dhandapani R, Krishnan PD, Zennifer A et al (2020) Additive manufacturing of biodegradable porous orthopaedic screw. Bioact Mater 5(3):458–467. https://doi.org/10.1016/j.bioactmat.2020.03.009

26. Xiong YZ, Wang W, Gao RN et al (2020) Fatigue behavior and osseointegration of porous Ti-6Al-4V scaffolds with dense core for dental application. Mater Des 195:108994. https://doi.org/10.1016/j.matdes.2020.108994

27. Li L, Shi JP, Zhang KJ et al (2019) Early osseointegration evaluation of porous Ti6Al4V scaffolds designed based on triply periodic minimal surface models. J Orthop Translat 19:94–105. https://doi.org/10.1016/j.jot.2019.03.003

28. Tsai PI, Chen CY, Huang SW et al (2018) Improvement of bone-tendon fixation by porous titanium interference screw: a rabbit animal model. J Orthop Res 36(10):2633–2640. https://doi.org/10.1002/jor.24037

29. Yang Y, Xu T, Bei HP et al (2022) Gaussian curvature-driven direction of cell fate toward osteogenesis with triply periodic minimal surface scaffolds. Proc Natl Acad Sci USA 119(41):e2206684119. https://doi.org/10.1073/pnas.2206684119

30. Gomez S, Vlad MD, Lopez J et al (2016) Design and properties of 3D scaffolds for bone tissue engineering. Acta Biomater 42:341–350. https://doi.org/10.1016/j.actbio.2016.06.032

31. Yao Y, Wang LZ, Li J et al (2020) A novel auxetic structure based bone screw design: tensile mechanical characterization and pull-out fixation strength evaluation. Mater Des 188:108424. https://doi.org/10.1016/j.matdes.2019.108424

32. Guo LX, Wang QD (2020) Biomechanical analysis of a new bilateral pedicle screw fixator system based on topological optimization. Int J Precis Eng Manuf 21(7):1363–1374. https://doi.org/10.1007/s12541-020-00336-6

33. Zhang AB, Chen H, Liu Y et al (2021) Customized reconstructive prosthesis design based on topological optimization to treat severe proximal tibia defect. Bio-Des Manuf 4(1):87–99. https://doi.org/10.1007/s42242-020-00102-7

34. Ernberg JJ, Asnis SE (1996) Materials and manufacturing of orthopaedic bone screws. In: Asnis SE, Kyle RF (Eds.), Cannulated Screw Fixation. Springer, New York, pp 1–14. https://doi.org/10.1007/978-1-4612-2326-9_1

35. Schlee M, van der Schoor WP, van der Schoor ARM (2015) Immediate loading of trabecular metal-enhanced titanium dental implants: interim results from an international proof-of-principle study. Clin Implant Dent Relat Res 17(51):e308–e320. https://doi.org/10.1111/cid.12127

36. Kapat K, Srivas PK, Rameshbabu AP et al (2017) Influence of porosity and pore-size distribution in Ti$_6$Al$_4$V foam on physicomechanical properties, osteogenesis, and quantitative validation of bone ingrowth by micro-computed tomography. ACS Appl Mater Interfaces 9(45):39235–39248. https://doi.org/10.1021/acsami.7b13960

37. Chang B, Song W, Han TX et al (2016) Influence of pore size of porous titanium fabricated by vacuum diffusion bonding of titanium meshes on cell penetration and bone ingrowth. Acta Biomater 33:311–321. https://doi.org/10.1016/j.actbio.2016.01.022

38. Kelly CN, Wang T, Crowley J et al (2021) High-strength, porous additively manufactured implants with optimized mechanical osseointegration. Biomaterials 279:121206. https://doi.org/10.1016/j.biomaterials.2021.121206

39. Benedetti M, Torresani E, Leoni M et al (2017) The effect of post-sintering treatments on the fatigue and biological behavior of Ti-6Al-4V ELI parts made by selective laser melting. J Mech Behav Biomed Mater 71:295–306. https://doi.org/10.1016/j.jmbbm.2017.03.024

40. Pei X, Wu LN, Zhou CC et al (2020) 3D printed titanium scaffolds with homogeneous diamond-like structures mimicking that of the osteocyte microenvironment and its bone regeneration study. Biofabrication 13(3):39501. https://doi.org/10.1088/1758-5090/abc060

41. Wu MW, Chen JK, Lin BH et al (2017) Improved fatigue endurance ratio of additive manufactured Ti-6Al-4V lattice by hot isostatic pressing. Mater Des 134:163–170. https://doi.org/10.1016/j.matdes.2017.08.048

42. Liu Q, Meng QK, Guo S et al (2013) α′ Type Ti–Nb–Zr alloys with ultra-low Young's modulus and high strength. Prog Nat Sci 23(6):562–565. https://doi.org/10.1016/j.pnsc.2013.11.005

43. Wang XJ, Xu SQ, Zhou SW et al (2016) Topological design and additive manufacturing of porous metals for bone scaffolds and orthopaedic implants: a review. Biomaterials 83:127–141. https://doi.org/10.1016/j.biomaterials.2016.01.012

44. Agarwal R, Gupta V, Singh J (2022) Additive manufacturing-based design approaches and challenges for orthopaedic bone screws: a state-of-the-art review. J Braz Soc Mech Sci Eng 44(1):37. https://doi.org/10.1007/s40430-021-03331-8

45. Becker W, Becker BE, Ricci A et al (2000) A prospective multicenter clinical trial comparing one- and two-stage titanium screw-shaped fixtures with one-stage plasma-sprayed solid-screw fixtures. Clin Implant Dent Relat Res 2(3):159–165. https://doi.org/10.1111/j.1708-8208.2000.tb00007.x

46. Mumcu E, Bilhan H, Cekici A (2011) Marginal bone loss around implants supporting fixed restorations. J Oral Implant 37(5):549–558. https://doi.org/10.1563/aaid-joi-d-10-00018

47. Joukar A, Kiapour A, Elgafy H et al (2020) Biomechanics of the sacroiliac joint: surgical treatments. Int J Spine Surg 14(3):355–367. https://doi.org/10.14444/7047

48. Mazur MD, Mahan MA, Shah LM et al (2017) Fate of S2-alar-iliac screws after 12-month minimum radiographic follow-up: preliminary results. Neurosurgery 80(1):67–72. https://doi.org/10.1227/NEU.0000000000001322

49. Tokuhashi Y, Matsuzaki H, Oda H et al (2008) Clinical course and significance of the clear zone around the pedicle screws in the lumbar degenerative disease. Spine 33(8):903–908. https://doi.org/10.1097/BRS.0b013e31816b1eff

50. Long WJ, Nayyar S, Chen KK et al (2018) Early aseptic loosening of the Tritanium primary acetabular component with screw fixation. Arthroplast Today 4(2):169–174. https://doi.org/10.1016/j.artd.2017.11.009

51. Sundaraj K, Salmon LJ, Heath EL et al (2020) Bioabsorbable versus titanium screws in anterior cruciate ligament reconstruction using hamstring autograft: a prospective, randomized controlled trial with 13-year follow-up. Am J Sports Med 48(6):1316–1326. https://doi.org/10.1177/0363546520911024

52. Taketomi S (2021) Editorial commentary: tunnel widening after anterior cruciate ligament reconstruction may increase laxity and complicate revision. Arthroscopy 37(8):2564–2566. https://doi.org/10.1016/j.arthro.2021.04.013

53. Putnis SE, Oshima T, Klasan A et al (2021) Adjustable suspension versus hybrid fixation in hamstring autograft anterior cruciate ligament reconstruction. Knee 28:1–8. https://doi.org/10.1016/j.knee.2020.10.014

54. Yang F, Chen C, Zhou QR et al (2017) Laser beam melting 3D printing of Ti6Al4V based porous structured dental implants: fabrication, biocompatibility analysis and photoelastic study. Sci Rep 7(1):45360. https://doi.org/10.1038/srep45360

55. Bhullar R, Habib A, Zhang KL et al (2019) Tunnel osteolysis post-ACL reconstruction: a systematic review examining select diagnostic modalities, treatment options and rehabilitation protocols. Knee Surg Sports Traumatol Arthrosc 27(2):524–533. https://doi.org/10.1007/s00167-018-5142-9

56. Szmukler-Moncler S, Piattelli A, Favero GA et al (2000) Considerations preliminary to the application of early and immediate loading protocols in dental implantology. Clin Oral Implant Res 11(1):12–25. https://doi.org/10.1034/j.1600-0501.2000.011001012.x

57. Im C, Park JH, Jeon YM et al (2022) Improvement of osseointegration of Ti-6Al-4V ELI alloy orthodontic mini-screws through anodization, cyclic pre-calcification, and heat treatments. Prog Orthod 23(1):11. https://doi.org/10.1186/s40510-022-00405-8

58. Fraser D, Funkenbusch P, Ercoli C et al (2020) Biomechanical analysis of the osseointegration of porous tantalum implants. J Prosthet Dent 123(6):811–820. https://doi.org/10.1016/j.prosdent.2019.09.014

59. Chang JZ, Tsai PI, Kuo MY et al (2019) Augmentation of DMLS biomimetic fental implants with weight-bearing strut to balance of biologic and mechanical demands: from bench to animal. Materials 12(1):164. https://doi.org/10.3390/ma12010164

60. Hoellwarth JS, Tetsworth K, Rozbruch SR et al (2020) Osseointegration for amputees: current implants, techniques, and future directions. JBJS Rev 8(3):e0043. https://doi.org/10.2106/JBJS.RVW.19.00043

61. Branemark R, Berlin O, Hagberg K et al (2014) A novel osseointegrated percutaneous prosthetic system for the treatment of patients with transfemoral amputation: a proprospective study of 51 patients. Bone Joint J 96B(1):106–113. https://doi.org/10.1302/0301-620x.96b1.31905

62. Heuberer PR, Brandl G, Pauzenberger L et al (2018) Radiological changes do not influence clinical mid-term outcome in stemless humeral head replacements with hollow screw fixation: a prospective radiological and clinical evaluation. BMC Musculoskelet Disord 19(1):28. https://doi.org/10.1186/s12891-018-1945-6

63. Alikhah A, Imiolczyk JP, Krukenberg A et al (2020) Screw fixation in stemless shoulder arthroplasty for the treatment of primary osteoarthritis leads to less osteolysis when compared to impaction fixation. BMC Musculoskelet Disord 21(1):295. https://doi.org/10.1186/s12891-020-03277-3

64. van der Schoor P, Schlee M, Wen HB (2022) Prospective pilot study of immediately provisionalized restorations of trabecular metal-enhanced titanium dental implants: a 5-year follow-up report. Appl Sci 12(3):942. https://doi.org/10.3390/app12030942

65. Spinato S, Zaffe D, Felice P et al (2014) A trabecular metal implant 4 months after placement: clinical-histologic case report. Implant Dent 23(1):3–7. https://doi.org/10.1097/ID.0000000000000020

66. Kim JT, Rudolf LM, Glaser JA (2013) Outcome of percutaneous sacroiliac joint fixation with porous plasma-coated triangular titanium implants: an independent review. Open Orthop J 7(1):51–56. https://doi.org/10.2174/1874325001307010051

67. Sachs D, Capobianco R (2013) Minimally invasive sacroiliac joint fusion: one-year outcomes in 40 patients. Adv Orthop 2013:536128. https://doi.org/10.1155/2013/536128

68. Rappoport LH, Luna IY, Joshua G (2017) Minimally invasive sacroiliac joint fusion using a novel hydroxyapatite-coated screw: preliminary 1-year clinical and radiographic results of a 2-year prospective study. World Neurosurg 101:493–497. https://doi.org/10.1016/j.wneu.2017.02.046

69. Williams AL, Gornet MF, Butkus JK (2005) CT evaluation of lumbar interbody fusion: current concepts. AJNR 26(8):2057–2066

70. Kuslich SD, Ulstrom CL, Griffith SL et al (1998) The Bagby and Kuslich method of lumbar interbody fusion: history, techniques, and 2-year follow-up results of a united states prospective, multicenter trial. Spine 23(11):1267–1279. https://doi.org/10.1097/00007632-199806010-00019

71. Nwankwo EC, Chen FY, Nettles DL et al (2019) Five-year follow-up of distal tibia bone and foot and ankle trauma treated with a 3D-printed titanium cage. Case Rep Orthop 2019:7571013. https://doi.org/10.1155/2019/7571013

72. El Chaar E, Castano A (2017) A retrospective survival study of trabecular tantalum implants immediately placed in posterior extraction sockets using a flapless technique. J Oral Implantol 43(2):114–124. https://doi.org/10.1563/aaid-joi-D-16-00071

73. Baeesa SS, Medrano BG, Noriega DC (2016) Long-term outcomes of posterior lumbar interbody fusion using stand-alone ray threaded cage for degenerative disk disease: a 20-year follow-up. Asian Spine J 10(6):1100–1105. https://doi.org/10.4184/asj.2016.10.6.1100

74. Nebergall A, Bragdon C, Antonellis A et al (2012) Stable fixation of an osseointegated implant system for above-the-knee amputees. Acta Orthop 83(2):121–128. https://doi.org/10.3109/17453674.2012.678799

75. Hawi N, Magosch P, Tauber M et al (2017) Nine-year outcome after anatomic stemless shoulder prosthesis: clinical and radiologic results. J Shoulder Elbow Surg 26(9):1609–1615. https://doi.org/10.1016/j.jse.2017.02.017

76. Bandyopadhyay A, Shivaram A, Tarafder S et al (2017) In vivo response of laser processed porous titanium implants for load-bearing implants. Ann Biomed Eng 45(1):249–260. https://doi.org/10.1007/s10439-016-1673-8

77. Xiu P, Jia ZJ, Lv J et al (2016) Tailored surface treatment of 3D printed porous Ti6Al4V by microarc oxidation for enhanced osseointegration via optimized bone in-growth patterns and

interlocked bone/implant interface. ACS Appl Mater Interfaces 8(28):17964–17975. https://doi.org/10.1021/acsami.6b05893

78. Huang CC, Li MJ, Tsai PI et al (2020) Novel design of additive manufactured hollow porous implants. Dent Mater 36(11):1437–1451. https://doi.org/10.1016/j.dental.2020.08.011

79. Duan YS, Liu XD, Zhang SJ et al (2020) Selective laser melted titanium implants play a positive role in early osseointegration in type 2 diabetes mellitus rats. Dent Mater J 39(2):214–221. https://doi.org/10.4012/dmj.2018-419

80. Rosa GL, Clienti C, Mineo R et al (2016) Experimental analysis of pedicle screws. In: 21st European Conference on Fracture, pp 1244–1251. https://doi.org/10.1016/j.prostr.2016.06.159

81. Lee BS, Lee HJ, Lee KS et al (2020) Enhanced osseointegration of Ti6Al4V ELI screws built-up by electron beam additive manufacturing: an experimental study in rabbits. Appl Surface Sci 508:145160. https://doi.org/10.1016/j.apsusc.2019.145160

82. Liang HX, Yang YW, Xie DQ et al (2019) Trabecular-like Ti-6Al-4V scaffolds for orthopedic: fabrication by selective laser melting and in vitro biocompatibility. J Mater Sci Technol 35(7):1284–1297. https://doi.org/10.1016/j.jmst.2019.01.012

83. Revell PA (2008) The combined role of wear particles, macrophages and lymphocytes in the loosening of total joint prostheses. J R Soc Interface 5(28):1263–1278. https://doi.org/10.1098/rsif.2008.0142

84. Sundfeldt M, Carlsson VL, Johansson BC et al (2006) Aseptic loosening, not only a question of wear: a review of different theories. Acta Orthop 77(2):177–197. https://doi.org/10.1080/17453670610045902

85. Song P, Hu C, Pei X et al (2019) Dual modulation of crystallinity and macro-/microstructures of 3D printed porous titanium implants to enhance stability and osseointegration. J Mater Chem B 7(17):2865–2877. https://doi.org/10.1039/c9tb00093c

86. Ahmadi SM, Kumar R, Borisov EV et al (2019) From microstructural design to surface engineering: a tailored approach for improving fatigue life of additively manufactured metabiomaterials. Acta Biomater 83:153–166. https://doi.org/10.1016/j.actbio.2018.10.043

87. Wang H, Su KX, Su LZ et al (2018) The effect of 3D-printed Ti$_6$Al$_4$V scaffolds with various macropore structures on osteointegration and osteogenesis: a biomechanical evaluation. J Mech Behav Biomed Mater 88:488–496. https://doi.org/10.1016/j.jmbbm.2018.08.049

88. Bai YX, Zhou R, Cao JY et al (2017) Microarc oxidation coating covered Ti implants with micro-scale gouges formed by a multistep treatment for improving osseointegration. Mater Sci Eng C 76:908–917. https://doi.org/10.1016/j.msec.2017.03.071

89. Wang N, Li H, Lu W et al (2011) Effects of TiO$_2$ nanotubes with different diameters on gene expression and osseointegration of implants in minipigs. Biomaterials 32(29):6900–6911. https://doi.org/10.1016/j.biomaterials.2011.06.023

90. Oh S, Daraio C, Chen LH et al (2006) Significantly accelerated osteoblast cell growth on aligned TiO$_2$ nanotubes. J Biomed Mater Res A 78(1):97–103. https://doi.org/10.1002/jbm.a.30722

91. He P, Zhang H, Li Y et al (2020) 1α,25-Dihydroxyvitamin D3-loaded hierarchical titanium scaffold enhanced early osseointegration. Mater Sci Eng C Mater Biol Appl 109:110551. https://doi.org/10.1016/j.msec.2019.110551

92. Li GL, Cao HL, Zhang WJ et al (2016) Enhanced osseointegration of hierarchical micro/nanotopographic titanium fabricated by microarc oxidation and electrochemical treatment. ACS Appl Mater Interfaces 8(6):3840–3852. https://doi.org/10.1021/acsami.5b10633

93. Huang JY, Li RQ, Yang JH et al (2021) Bioadaptation of implants to in vitro and in vivo oxidative stress pathological conditions via nanotopography-induced FoxO1 signaling pathways to enhance

Osteoimmunal regeneration. Bioactive Mater 6(10):3164–3176. https://doi.org/10.1016/j.bioactmat.2021.02.023

94. Su EP, Justin DF, Pratt CR et al (2018) Effects of titanium nanotubes on the osseointegration, cell differentiation, mineralisation and antibacterial properties of orthopaedic implant surfaces. Bone Joint J 100B(1):9–16. https://doi.org/10.1302/0301-620x.100b1.Bjj-2017-0551.R1

95. Yan CZ, Hao L, Hussein A et al (2017) Microstructural and surface modifications and hydroxyapatite coating of Ti-6Al-4V triply periodic minimal surface lattices fabricated by selective laser melting. Mater Sci Eng C Mater Biol Appl 75:1515–1524. https://doi.org/10.1016/j.msec.2017.03.066

96. Vantaggiato G, Iezzi G, Fiera E et al (2008) Histologic and histomorphometric report of three immediately loaded screw implants retrieved from man after a three-year loading period. Implant Dent 17(2):192–199. https://doi.org/10.1097/ID.0b013e318166d654

97. Huang YM, Huang CC, Tsai PI et al (2020) Three-dimensional printed porous titanium screw with bioactive surface modification for bone-tendon healing: a rabbit animal model. Int J Mol Sci 21(10):3628. https://doi.org/10.3390/ijms21103628

98. Lee JK, Choi DS, Jang I et al (2015) Improved osseointegration of dental titanium implants by TiO$_2$ nanotube arrays with recombinant human bone morphogenetic protein-2: a pilot in vivo study. Int J Nanomedicine 10:1145–1154. https://doi.org/10.2147/IJN.S78138

99. Zhao X, You L, Wang T et al (2020) Enhanced osseointegration of titanium implants by surface modification with silicon-doped titania nanotubes. Int J Nanomed 15:8583–8594. https://doi.org/10.2147/IJN.S270311

100. Xiang YM, Liu XM, Mao CY et al (2018) Infection-prevention on Ti implants by controlled drug release from folic acid/ZnO quantum dots sealed titania nanotubes. Mater Sci Eng C Mater Biol Appl 85:214–224. https://doi.org/10.1016/j.msec.2017.12.034

101. Arcos D, Vallet-Regí M (2020) Substituted hydroxyapatite coatings of bone implants. J Mater Chem B 8(9):1781–1800. https://doi.org/10.1039/C9TB02710F

102. Bakin B, Delice TK, Tiric U et al (2016) Bioactivity and corrosion properties of magnesium-substituted CaP coatings produced via electrochemical deposition. Surf Coat Tech 301:29–35. https://doi.org/10.1016/j.surfcoat.2015.12.078

103. Fielding GA, Roy M, Bandyopadhyay A et al (2012) Antibacterial and biological characteristics of silver containing and strontium doped plasma sprayed hydroxyapatite coatings. Acta Biomater 8(8):3144–3152. https://doi.org/10.1016/j.actbio.2012.04.004

104. Yamaguchi M, Oishi H, Suketa Y (1987) Stimulatory effect of zinc on bone formation in tissue culture. Biochem Pharmacol 36(22):4007–4012. https://doi.org/10.1016/0006-2952(87)90471-0

105. Stanić V, Dimitrijević S, Antić-Stanković J et al (2010) Synthesis, characterization and antimicrobial activity of copper and zinc-doped hydroxyapatite nanopowders. Appl Surf Sci 256(20):6083–6089. https://doi.org/10.1016/j.apsusc.2010.03.124

106. Utku FS, Seckin E, Goller G et al (2014) Carbonated hydroxyapatite deposition at physiological temperature on ordered titanium oxide nanotubes using pulsed electrochemistry. Ceram Int 40(10):15479–15487. https://doi.org/10.1016/j.ceramint.2014.07.004

107. Wang J, Chao YJ, Wan QB et al (2009) Fluoridated hydroxyapatite coatings on titanium obtained by electrochemical deposition. Acta Biomater 5(5):1798–1807. https://doi.org/10.1016/j.actbio.2009.01.005

108. Geng Z, Wang RF, Zhuo XL et al (2017) Incorporation of silver and strontium in hydroxyapatite coating on titanium surface for enhanced antibacterial and biological properties. Mater Sci Eng C 71:852–861. https://doi.org/10.1016/j.msec.2016.10.079

109. Qiao HX, Zou QS, Yuan CF et al (2018) Composite coatings of lanthanum-doped fluor-hydroxyapatite and a layer of strontium titanate nanotubes: fabrication, bio-corrosion resistance, cytocompatibility and osteogenic differentiation. Ceram Int 44(14):16632–16646. https://doi.org/10.1016/j.ceramint.2018.06.090

110. Luo JJ, Tamaddon M, Yan CY et al (2020) Improving the fretting biocorrosion of Ti$_6$Al$_4$V alloy bone screw by decorating structure optimised TiO$_2$ nanotubes layer. J Mater Sci Technol 49:47–55. https://doi.org/10.1016/j.jmst.2020.02.027

111. Li JL, Wang S, Cao F et al (2019) Fabrication and characterization of nanopillar-like HA coating on porous Ti6Al4V scaffold by a combination of alkali–acid-heat and hydrothermal treatments. Acta Metall Sin Engl Lett 32(9):1075–1088. https://doi.org/10.1007/s40195-019-00920-4

112. Yin S, Zhang WJ, Tang YM et al (2021) Preservation of alveolar ridge height through mechanical memory: a novel dental implant design. Bioact Mater 6(1):75–83. https://doi.org/10.1016/j.bioactmat.2020.07.015

113. Lian MF, Sun BB, Han Y et al (2021) A low-temperature-printed hierarchical porous sponge-like scaffold that promotes cell-material interaction and modulates paracrine activity of MSCs for vascularized bone regeneration. Biomaterials 274:120841. https://doi.org/10.1016/j.biomaterials.2021.120841

114. Hedayati R, Sadighi M, Mohammadi-Aghdam M et al (2016) Mechanical properties of regular porous biomaterials made from truncated cube repeating unit cells: analytical solutions and computational models. Mater Sci Eng C Mater Biol Appl 60:163–183. https://doi.org/10.1016/j.msec.2015.11.001

115. Al-Ketan O, Rowshan R, Abu Al-Rub RK (2018) Topology-mechanical property relationship of 3D printed strut, skeletal, and sheet based periodic metallic cellular materials. Addit Manuf 19:167–183. https://doi.org/10.1016/j.addma.2017.12.006

116. Yuan L, Ding SL, Wen C (2019) Additive manufacturing technology for porous metal implant applications and triple minimal surface structures: a review. Bioact Mater 4(1):56–70. https://doi.org/10.1016/j.bioactmat.2018.12.003

117. Mirkhalaf M, Wang X, Entezari A et al (2021) Redefining architectural effects in 3D printed scaffolds through rational design for optimal bone tissue regeneration. Appl Mater Today 25:101168. https://doi.org/10.1016/j.apmt.2021.101168

118. Kelly CN, Francovich J, Julmi S et al (2019) Fatigue behavior of as-built selective laser melted titanium scaffolds with sheet-based gyroid microarchitecture for bone tissue engineering. Acta Biomater 94:610–626. https://doi.org/10.1016/j.actbio.2019.05.046

119. Zadpoor AA (2019) Mechanical performance of additively manufactured meta-biomaterials. Acta Biomater 85:41–59. https://doi.org/10.1016/j.actbio.2018.12.038

120. Gibson LJ, Ashby MF (1997) Cellular solids: structure and properties. Cambridge University Press, UK. https://doi.org/10.1017/CBO9781139878326

121. Ashby MF (2006) The properties of foams and lattices. Philos Trans Math Phys Eng Sci 364(1838):15–30. https://doi.org/10.1098/rsta.2005.1678

122. Fousova M, Vojtech D, Kubasek J et al (2017) Promising characteristics of gradient porosity Ti-6Al-4V alloy prepared by SLM process. J Mech Behav Biomed Mater 69:368–376. https://doi.org/10.1016/j.jmbbm.2017.01.043

123. Zhang S, Wei QS, Cheng LY et al (2014) Effects of scan line spacing on pore characteristics and mechanical properties of porous Ti6Al4V implants fabricated by selective laser melting. Mater Des 63:185–193. https://doi.org/10.1016/j.matdes.2014.05.021

124. Deshpande VS, Ashby MF, Fleck NA (2001) Foam topology: bending versus stretching dominated architectures. Acta Mater 49(6):1035–1040. https://doi.org/10.1016/S1359-6454(00)00379-7

125. Yang L, Han CJ, Wu HZ et al (2020) Insights into unit cell size effect on mechanical responses and energy absorption capability of titanium graded porous structures manufactured by laser powder bed fusion. J Mech Behav Biomed Mater 109:103843. https://doi.org/10.1016/j.jmbbm.2020.103843

126. Ran QC, Yang WH, Hu Y et al (2018) Osteogenesis of 3D printed porous Ti6Al4V implants with different pore sizes. J Mech Behav Biomed Mater 84:1–11. https://doi.org/10.1016/j.jmbbm.2018.04.010

127. Taniguchi N, Fujibayashi S, Takemoto M et al (2016) Effect of pore size on bone ingrowth into porous titanium implants fabricated by additive manufacturing: an in vivo experiment. Mater Sci Eng C Mater Biol Appl 59:690–701. https://doi.org/10.1016/j.msec.2015.10.069

128. Davoodi E, Montazerian H, Esmaeilizadeh R et al (2021) Additively manufactured gradient porous Ti-6Al-4V hip replacement implants embedded with cell-laden gelatin methacryloyl hydrogels. ACS Appl Mater Interfaces 13(19):22110–22123. https://doi.org/10.1021/acsami.0c20751

129. Poumarat G, Squire P (1993) Comparison of mechanical properties of human, bovine bone and a new processed bone xenograft. Biomaterials 14(5):337–340. https://doi.org/10.1016/0142-9612(93)90051-3

130. Zysset PK, Guo XE, Hoffler CE et al (1999) Elastic modulus and hardness of cortical and trabecular bone lamellae measured by nanoindentation in the human femur. J Biomech 32(10):1005–1012. https://doi.org/10.1016/s0021-9290(99)00111-6

131. Goldstein SA, Wilson DL, Sonstegard DA et al (1983) The mechanical properties of human tibial trabecular bone as a function of metaphyseal location. J Biomech 16(12):965–969. https://doi.org/10.1016/0021-9290(83)90097-0

132. Frost HM (2004) A 2003 update of bone physiology and Wolff's law for clinicians. Angle Orthod 74(1):3–15

133. Hara D, Nakashima Y, Sato T et al (2016) Bone bonding strength of diamond-structured porous titanium-alloy implants manufactured using the electron beam-melting technique. Mater Sci Eng C Mater Biol Appl 59:1047–1052. https://doi.org/10.1016/j.msec.2015.11.025

134. Zhao Z, Li JC, Wei Y et al (2022) Design and properties of graded polyamide12/hydroxyapatite scaffolds based on primitive lattices using selective laser sintering. J Mech Behav Biomed Mater 126:105052. https://doi.org/10.1016/j.jmbbm.2021.105052

135. Cheng A, Humayun A, Cohen DJ et al (2014) Additively manufactured 3D porous Ti-6Al-4V constructs mimic trabecular bone structure and regulate osteoblast proliferation, differentiation and local factor production in a porosity and surface roughness dependent manner. Biofabrication 6(4):045007. https://doi.org/10.1088/1758-5082/6/4/045007

136. Chen ZY, Yan XC, Yin S et al (2020) Influence of the pore size and porosity of selective laser melted Ti6Al4V ELI porous scaffold on cell proliferation, osteogenesis and bone ingrowth. Mater Sci Eng C Mater Biol Appl 106:110289. https://doi.org/10.1016/j.msec.2019.110289

137. Shah FA, Snis A, Matic A et al (2016) 3D printed Ti6Al4V implant surface promotes bone maturation and retains a higher density of less aged osteocytes at the bone-implant interface. Acta Biomater 30:357–367. https://doi.org/10.1016/j.actbio.2015.11.013

138. Bobbert FSL, Lietaert K, Eftekhari AA et al (2017) Additively manufactured metallic porous biomaterials based on minimal surfaces: a unique combination of topological, mechanical, and mass transport properties. Acta Biomater 53:572–584. https://doi.org/10.1016/j.actbio.2017.02.024

139. Hulbert SF, Young FA, Mathews RS et al (1970) Potential of ceramic materials as permanently implantable skeletal prostheses.

J Biomed Mater Res 4(3):433–456. https://doi.org/10.1002/jbm.820040309

140. Osorio M, Fernandez-Morales P, Ganan P et al (2019) Development of novel three-dimensional scaffolds based on bacterial nanocellulose for tissue engineering and regenerative medicine: effect of processing methods, pore size, and surface area. J Biomed Mater Res A 107(2):348–359. https://doi.org/10.1002/jbm.a.36532

141. Fukuda A, Takemoto M, Saito T et al (2011) Osteoinduction of porous Ti implants with a channel structure fabricated by selective laser melting. Acta Biomater 7(5):2327–2336. https://doi.org/10.1016/j.actbio.2011.01.037

142. Yang E, Leary M, Lozanovski B et al (2019) Effect of geometry on the mechanical properties of Ti-6Al-4V Gyroid structures fabricated via SLM: a numerical study. Mater Des 184:108165. https://doi.org/10.1016/j.matdes.2019.108165

143. Abu Al-Rub RK, Lee DW, Khan KA et al (2020) Effective anisotropic elastic and plastic yield properties of periodic foams derived from triply periodic Schoen's I-WP minimal surface. J Eng Mech 146(5):04020030. https://doi.org/10.1061/(asce)em.1943-7889.0001759

144. Al-Ketan O, Lee DW, Rowshan R et al (2020) Functionally graded and multi-morphology sheet TPMS lattices: design, manufacturing, and mechanical properties. J Mech Behav Biomed Mater 102:103520. https://doi.org/10.1016/j.jmbbm.2019.103520

145. Yan CZ, Hao L, Hussein A et al (2014) Advanced lightweight 316L stainless steel cellular lattice structures fabricated via selective laser melting. Mater Des 55:533–541. https://doi.org/10.1016/j.matdes.2013.10.027

146. Barba D, Alabort E, Reed RC (2019) Synthetic bone: design by additive manufacturing. Acta Biomater 97:637–656. https://doi.org/10.1016/j.actbio.2019.07.049

147. Vijayavenkataraman S, Kuan LY, Lu WF (2020) 3D-printed ceramic triply periodic minimal surface structures for design of functionally graded bone implants. Mater Des 191:108602. https://doi.org/10.1016/j.matdes.2020.108602

148. Cai ZZ, Liu ZH, Hu XD et al (2019) The effect of porosity on the mechanical properties of 3D-printed triply periodic minimal surface (TPMS) bioscaffold. Bio-Des Manuf 2(4):242–255. https://doi.org/10.1007/s42242-019-00054-7

149. Hailu YM, Nazir A, Hsu CP et al (2022) Investigation of torsional properties of surface- and strut-based lattice structures manufactured using multiJet fusion technology. Int J Adv Manuf Technol 119(9–10):5929–5945. https://doi.org/10.1007/s00170-022-08681-8

150. Novak N, Al-Ketan O, Krstulovic-Opara L et al (2022) Bending behavior of triply periodic minimal surface foam-filled tubes. Mech Adv Mater Struct 30(15):3061–3074. https://doi.org/10.1080/15376494.2022.2068207

151. Peng CX, Fox K, Qian M et al (2021) 3D printed sandwich beams with bioinspired cores: mechanical performance and modelling. Thin Wall Struct 161:107471. https://doi.org/10.1016/j.tws.2021.107471

152. Yang L, Li Y, Chen Y et al (2022) Topologically optimized lattice structures with superior fatigue performance. Int J Fatigue 165:107188. https://doi.org/10.1016/j.ijfatigue.2022.107188

153. Yang L, Yan CZ, Cao WC et al (2019) Compression–compression fatigue behaviour of gyroid-type triply periodic minimal surface porous structures fabricated by selective laser melting. Acta Mater 181:49–66. https://doi.org/10.1016/j.actamat.2019.09.042

154. Vu AA, Burke DA, Bandyopadhyay A et al (2021) Effects of surface area and topography on 3D printed tricalcium phosphate scaffolds for bone grafting applications. Addit Manuf 39:101870. https://doi.org/10.1016/j.addma.2021.101870

155. Hauge EM, Qvesel D, Eriksen EF et al (2001) Cancellous bone remodeling occurs in specialized compartments lined by cells expressing osteoblastic markers. J Bone Miner Res 16(9):1575–1582. https://doi.org/10.1359/jbmr.2001.16.9.1575

156. Gamsjäger E, Bidan CM, Fischer FD et al (2013) Modelling the role of surface stress on the kinetics of tissue growth in confined geometries. Acta Biomater 9(3):5531–5543. https://doi.org/10.1016/j.actbio.2012.10.020

157. Dunlop JWC, Fischer FD, Gamsjäger E et al (2010) A theoretical model for tissue growth in confined geometries. J Mech Phys Solids 58(8):1073–1087. https://doi.org/10.1016/j.jmps.2010.04.008

158. Zhang Q, Ma LM, Ji XF et al (2022) High-strength hydroxyapatite scaffolds with minimal surface macrostructures for load-bearing bone regeneration. Adv Funct Mater 32(33):2204182. https://doi.org/10.1002/adfm.202204182

159. Fantini M, Curto M, De Crescenzio F (2016) A method to design biomimetic scaffolds for bone tissue engineering based on Voronoi lattices. Virt Phys Proto ty 11(2):77–90. https://doi.org/10.1080/17452759.2016.1172301

160. Fantini M, Curto M (2017) Interactive design and manufacturing of a Voronoi-based biomimetic bone scaffold for morphological characterization. Int J Interact Des Manuf 12(2):585–596. https://doi.org/10.1007/s12008-017-0416-x

161. Zhu L, Liang HX, Lv F et al (2021) Design and compressive fatigue properties of irregular porous scaffolds for orthopedics fabricated using selective laser melting. ACS Biomater Sci Eng 7(4):1663–1672. https://doi.org/10.1021/acsbiomaterials.0c01392

162. Wang GJ, Shen LD, Zhao JF et al (2018) Design and compressive behavior of controllable irregular porous scaffolds: based on Voronoi-tessellation and for additive manufacturing. ACS Biomater Sci Eng 4(2):719–727. https://doi.org/10.1021/acsbiomaterials.7b00916

163. Chen H, Liu Y, Wang CY et al (2021) Design and properties of biomimetic irregular scaffolds for bone tissue engineering. Comput Biol Med 130:104241. https://doi.org/10.1016/j.compbiomed.2021.104241

164. Entezari A, Roohani I, Li GL et al (2019) Architectural design of 3D printed scaffolds controls the volume and functionality of newly formed bone. Adv Healthc Mater 8(1):e1801353. https://doi.org/10.1002/adhm.201801353

165. Wang C, Xu DL, Lin L et al (2021) Large-pore-size Ti6Al4V scaffolds with different pore structures for vascularized bone regeneration. Mater Sci Eng C Mater Biol Appl 131:112499. https://doi.org/10.1016/j.msec.2021.112499

166. Ragone V, Canciani E, Arosio M et al (2020) In vivo osseointegration of a randomized trabecular titanium structure obtained by an additive manufacturing technique. J Mater Sci Mater Med 31(2):17. https://doi.org/10.1007/s10856-019-6357-0

167. Wu WW, Hu WX, Qian GA et al (2019) Mechanical design and multifunctional applications of chiral mechanical metamaterials: a review. Mater Des 180:107950. https://doi.org/10.1016/j.matdes.2019.107950

168. Schwerdtfeger J, Schury F, Stingl M et al (2012) Mechanical characterisation of a periodic auxetic structure produced by SEBM. Phys Status Solidi B Basic Res 249(7):1347–1352. https://doi.org/10.1002/pssb.201084211

169. Gao Q, Tan CA, Hulbert G et al (2020) Geometrically nonlinear mechanical properties of auxetic double-V microstructures with negative Poisson's ratio. Eur J Mech A Solids 80:103933. https://doi.org/10.1016/j.euromechsol.2019.103933

170. Chen JP, Chen WS, Hao H et al (2020) Mechanical behaviors of 3D re-entrant honeycomb polyamide structure under compression. Mater Today Commun 24:101062. https://doi.org/10.1016/j.mtcomm.2020.101062

171. Wang ZW, Luan CC, Liao GX et al (2020) Progress in auxetic mechanical metamaterials: structures, characteristics,

✷ Springer

manufacturing methods, and applications. Adv Eng Mater 22(10):2000312. https://doi.org/10.1002/adem.202000312

172. Yao Y, Yuan H, Huang HW et al (2021) Biomechanical design and analysis of auxetic pedicle screw to resist loosening. Comput Biol Med 133:104386. https://doi.org/10.1016/j.compbiomed.2021.104386

173. Kolken HMA, Janbaz S, Leeflang SMA et al (2018) Rationally designed meta-implants: a combination of auxetic and conventional meta-biomaterials. Mater Horiz 5(1):28–35. https://doi.org/10.1039/c7mh00699c

174. Frenzel T, Kadic M, Wegener M (2017) Three-dimensional mechanical metamaterials with a twist. Science 358(6366):1072–1074. https://doi.org/10.1126/science.aao4640

175. Wang YL, Zhao WZ, Zhou G et al (2018) Suspension mechanical performance and vehicle ride comfort applying a novel jounce bumper based on negative Poisson's ratio structure. Adv Eng Softw 122:1–12. https://doi.org/10.1016/j.advengsoft.2018.04.001

176. Yang L, Cormier D, West H et al (2012) Non-stochastic Ti–6Al–4V foam structures with negative Poisson's ratio. Mater Sci Eng A 558:579–585. https://doi.org/10.1016/j.msea.2012.08.053

177. Bezazi A, Boukharouba W, Scarpa F (2009) Mechanical properties of auxetic carbon/epoxy composites: static and cyclic fatigue behaviour. Phys Status Solidi B Basic Res 246(9):2102–2110. https://doi.org/10.1002/pssb.200982042

178. Yang S, Chalivendra VB, Kim YK (2017) Fracture and impact characterization of novel auxetic Kevlar®/Epoxy laminated composites. Compos Struct 168:120–129. https://doi.org/10.1016/j.compstruct.2017.02.034

179. Jiang H, Zhang ZN, Chen YY (2020) 3D printed tubular lattice metamaterials with engineered mechanical performance. Appl Phys Lett 117(1):011906. https://doi.org/10.1063/5.0014932

180. Jiang H, Ziegler H, Zhang ZN et al (2022) Bending behavior of 3D printed mechanically robust tubular lattice metamaterials. Addit Manuf 50:102565. https://doi.org/10.1016/j.addma.2021.102565

181. Yang L, Harrysson O, West H et al (2012) Compressive properties of Ti–6Al–4V auxetic mesh structures made by electron beam melting. Acta Mater 60(8):3370–3379. https://doi.org/10.1016/j.actamat.2012.03.015

182. Gao Q, Zhao X, Wang CZ et al (2018) Multi-objective crashworthiness optimization for an auxetic cylindrical structure under axial impact loading. Mater Des 143:120–130. https://doi.org/10.1016/j.matdes.2018.01.063

183. Yang H, Wang B, Ma L (2019) Mechanical properties of 3D double-U auxetic structures. Int J Solid Struct 180–181:13–29. https://doi.org/10.1016/j.ijsolstr.2019.07.007

184. Guo MF, Yang H, Ma L (2020) Design and analysis of 2D double-U auxetic honeycombs. Thin Wall Struct 155:106915. https://doi.org/10.1016/j.tws.2020.106915

185. Meena K, Singamneni S (2019) A new auxetic structure with significantly reduced stress concentration effects. Mater Des 173:107779. https://doi.org/10.1016/j.matdes.2019.107779

186. Warmuth F, Osmanlic F, Adler L et al (2017) Fabrication and characterisation of a fully auxetic 3D lattice structure via selective electron beam melting. Smart Mater Struct 26(2):25013. https://doi.org/10.1088/1361-665x/26/2/025013

187. Ma C, Lei HS, Liang J et al (2018) Macroscopic mechanical response of chiral-type cylindrical metastructures under axial compression loading. Mater Des 158:198–212. https://doi.org/10.1016/j.matdes.2018.08.022

188. Huiskes R, Weinans H, Grootenboer HJ et al (1987) Adaptive bone-remodeling theory applied to prosthetic-design analysis. J Biomech 20(11–12):1135–1150. https://doi.org/10.1016/0021-9290(87)90030-3

189. Zhu JJ, Marshall B, Tang X et al (2022) ACL graft with extra-cortical fixation rotates around the femoral tunnel aperture during knee flexion. Knee Surg Sports Traumatol Arthrosc 30(1):116–123. https://doi.org/10.1007/s00167-021-06703-8

190. Wang LZ, Huang HW, Yuan H et al (2023) In vitro fatigue behavior and in vivo osseointegration of the auxetic porous bone screw. Acta Biomater 170:185–201. https://doi.org/10.1016/j.actbio.2023.08.040

191. Lee JJ, Ng HY, Lin YH et al (2022) The synergistic effect of cyclic tensile force and periodontal ligament cell-laden calcium silicate/gelatin methacrylate auxetic hydrogel scaffolds for bone regeneration. Cells 11(13):2069. https://doi.org/10.3390/cells11132069

192. Li ZH, Müller R, Ruffoni D (2018) Bone remodeling and mechanobiology around implants: insights from small animal imaging. J Orthop Res 36(2):584–593. https://doi.org/10.1002/jor.23758

193. Hazlehurst KB, Wang CJ, Stanford M (2014) An investigation into the flexural characteristics of functionally graded cobalt chrome femoral stems manufactured using selective laser melting. Mater Des 60:177–183. https://doi.org/10.1016/j.matdes.2014.03.068

194. Hailu YM, Nazir A, Lin SC et al (2021) The effect of functional gradient material distribution and patterning on torsional properties of lattice structures manufactured using multiJet fusion technology. Materials 14(21):6521. https://doi.org/10.3390/ma14216521

195. Zhang JF, Chen XH, Sun YX et al (2022) Design of a biomimetic graded TPMS scaffold with quantitatively adjustable pore size. Mater Des 218:110665. https://doi.org/10.1016/j.matdes.2022.110665

196. Tan CL, Deng C, Li S et al (2022) Mechanical property and biological behaviour of additive manufactured TiNi functionally graded lattice structure. Int J Extreme Manuf 4(4):45003. https://doi.org/10.1088/2631-7990/ac94fa

197. Zhao S, Li SJ, Wang SG et al (2018) Compressive and fatigue behavior of functionally graded Ti-6Al-4V meshes fabricated by electron beam melting. Acta Mater 150:1–15. https://doi.org/10.1016/j.actamat.2018.02.060

198. Liu Y, Zhang AB, Wang CY et al (2020) Biomechanical comparison between metal block and cement-screw techniques for the treatment of tibial bone defects in total knee arthroplasty based on finite element analysis. Comput Biol Med 125:104006. https://doi.org/10.1016/j.compbiomed.2020.104006

199. Song CJ, Chang HR, Zhang D et al (2021) Biomechanical evaluation of oblique lumbar interbody fusion with various fixation options: a finite element analysis. Orthop Surg 13(2):517–529. https://doi.org/10.1111/os.12877

200. Zeng W, Liu Y, Hou X (2020) Biomechanical evaluation of internal fixation implants for femoral neck fractures: a comparative finite element analysis. Comput Meth Prog Bio 196:105714. https://doi.org/10.1016/j.cmpb.2020.105714

201. Lin HM, Liu CL, Pan YN et al (2014) Biomechanical analysis and design of a dynamic spinal fixator using topology optimization: a finite element analysis. Med Biol Eng Comput 52(5):499–508. https://doi.org/10.1007/s11517-014-1154-x

202. Fu J, Li H, Song X et al (2022) Multi-scale defects in powder-based additively manufactured metals and alloys. J Mater Sci Technol 122:165–199. https://doi.org/10.1016/j.jmst.2022.02.015

203. Wally ZJ, Haque AM, Feteira A et al (2019) Selective laser melting processed Ti6Al4V lattices with graded porosities for dental applications. J Mech Behav Biomed Mater 90:20–29. https://doi.org/10.1016/j.jmbbm.2018.08.047

204. Yan CZ, Hao L, Hussein A et al (2015) Ti-6Al-4V triply periodic minimal surface structures for bone implants fabricated via

selective laser melting. J Mech Behav Biomed Mater 51:61–73. https://doi.org/10.1016/j.jmbbm.2015.06.024

205. Shang C, Wang CY, Li CF et al (2020) Eliminating the crack of laser 3D printed functionally graded material from TA15 to Inconel718 by base preheating. Opt Laser Technol 126:106100. https://doi.org/10.1016/j.optlastec.2020.106100

206. Ali H, Ma L, Ghadbeigi H et al (2017) In-situ residual stress reduction, martensitic decomposition and mechanical properties enhancement through high temperature powder bed pre-heating of selective laser melted Ti6Al4V. Mater Sci Eng A 695:211–220. https://doi.org/10.1016/j.msea.2017.04.033

207. Polozov I, Sufiiarov V, Kantyukov A et al (2020) Microstructure, densification, and mechanical properties of titanium intermetallic alloy manufactured by laser powder bed fusion additive manufacturing with high-temperature preheating using gas atomized and mechanically alloyed plasma spheroidized powders. Addit Manuf 34:101374. https://doi.org/10.1016/j.addma.2020.101374

208. Saedi S, Shayesteh Moghaddam N, Amerinatanzi A et al (2018) On the effects of selective laser melting process parameters on microstructure and thermomechanical response of Ni-rich NiTi. Acta Mater 144:552–560. https://doi.org/10.1016/j.actamat.2017.10.072

209. Huang QL, Liu XJ, Yang X et al (2015) Specific heat treatment of selective laser melted Ti-6Al-4V for biomedical applications. Front Mater Sci 9(4):373–381. https://doi.org/10.1007/s11706-015-0315-7

210. Yuan W, Hou WT, Li SJ et al (2018) Heat treatment enhancing the compressive fatigue properties of open-cellular Ti-6Al-4V alloy prototypes fabricated by electron beam melting. J Mater Sci Technol 34(7):1127–1131. https://doi.org/10.1016/j.jmst.2017.12.003

211. Jam A, du Plessis A, Lora C et al (2022) Manufacturability of lattice structures fabricated by laser powder bed fusion: a novel biomedical application of the beta Ti-21S alloy. Addit Manuf 50:102556. https://doi.org/10.1016/j.addma.2021.102556

212. Banerjee D, Williams JC (2013) Perspectives on titanium science and technology. Acta Mater 61(3):844–879. https://doi.org/10.1016/j.actamat.2012.10.043

213. Liu YJ, Li SJ, Wang HL et al (2016) Microstructure, defects and mechanical behavior of beta-type titanium porous structures manufactured by electron beam melting and selective laser melting. Acta Mater 113:56–67. https://doi.org/10.1016/j.actamat.2016.04.029

214. Zhou YL, Niinomi M (2009) Ti–25Ta alloy with the best mechanical compatibility in Ti–Ta alloys for biomedical applications. Mater Sci Eng C 29(3):1061–1065. https://doi.org/10.1016/j.msec.2008.09.012

215. Semlitsch M, Weber H, Streicher RM et al (1991) Joint prostheses components of warm-forged and surface treated Ti-6Al-7Nb alloy. Biomed Tech Biomed Eng 36(5):112–119. https://doi.org/10.1515/bmte.1991.36.5.112

216. Vasilescu C, Drob SI, Osiceanu P et al (2015) Surface analysis, microstructural, mechanical and electrochemical properties of new Ti-15Ta-5Zr alloy. Metal Mater Int 21(2):242–250. https://doi.org/10.1007/s12540-015-4074-x

217. Popa M, Vasilescu E, Drob P et al (2012) Microstructure, mechanical, and anticorrosive properties of a new Ti-20Nb-10Zr-5Ta alloy based on nontoxic and nonallergenic elements. Metal Mater Int 18(4):639–645. https://doi.org/10.1007/s12540-012-4026-7

218. Luo JP, Sun JF, Huang YJ et al (2019) Low-modulus biomedical Ti-30Nb-5Ta-3Zr additively manufactured by selective laser melting and its biocompatibility. Mater Sci Eng C Mater Biol Appl 97:275–284. https://doi.org/10.1016/j.msec.2018.11.077

219. Pellizzari M, Jam A, Tschon M et al (2020) A 3D-printed ultra-low Young's modulus β-Ti alloy for biomedical applications. Materials 13(12):2792. https://doi.org/10.3390/ma13122792

220. Windhagen H, Radtke K, Weizbauer A et al (2013) Biodegradable magnesium-based screw clinically equivalent to titanium screw in hallux valgus surgery: short term results of the first prospective, randomized, controlled clinical pilot study. Biomed Eng Online 12:62. https://doi.org/10.1186/1475-925x-12-62

221. Sturznickel J, Delsmann MM, Jungesblut OD et al (2021) Safety and performance of biodegradable magnesium-based implants in children and adolescents. Injury 52(8):2265–2271. https://doi.org/10.1016/j.injury.2021.03.037

222. Wong TT, Denning J, Moy MP et al (2021) MRI following medial patellofemoral ligament reconstruction: assessment of imaging features found with post-operative pain, arthritis, and graft failure. Skeletal Radiol 50(5):981–991. https://doi.org/10.1007/s00256-020-03655-x

223. Zhang XT, Mao J, Zhou YF et al (2020) Mechanical properties and osteoblast proliferation of complex porous dental implants filled with magnesium alloy based on 3D printing. J Biomater Appl 35(10):1275–1283. https://doi.org/10.1177/0885328220957902

224. Liu WC, Chang CH, Chen CH et al (2022) 3D-printed double-helical biodegradable iron suture anchor: a rabbit rotator cuff tear model. Materials 15(8):2801. https://doi.org/10.3390/ma15082801

225. Qu XH, Yang HT, Jia B et al (2021) Zinc alloy-based bone internal fixation screw with antibacterial and anti-osteolytic properties. Bioact Mater 6(12):4607–4624. https://doi.org/10.1016/j.bioactmat.2021.05.023

226. Tai CC, Lo HL, Liaw CK et al (2021) Biocompatibility and biological performance evaluation of additive-manufactured bioabsorbable iron-based porous suture anchor in a rabbit model. Int J Mol Sci 22(14):7368. https://doi.org/10.3390/ijms22147368

227. Prasad K, Bazaka O, Chua M et al (2017) Metallic biomaterials: current challenges and opportunities. Materials 10(8):884. https://doi.org/10.3390/ma10080884

228. Yang H, Jia B, Zhang Z et al (2020) Alloying design of biodegradable zinc as promising bone implants for load-bearing applications. Nat Commun 11(1):401. https://doi.org/10.1038/s41467-019-14153-7

229. Montani M, Demir AG, Mostaed E et al (2017) Processability of pure Zn and pure Fe by SLM for biodegradable metallic implant manufacturing. Rapid Prototyping J 23(3):514–523. https://doi.org/10.1108/rpj-08-2015-0100

230. Wen P, Voshage M, Jauer L et al (2018) Laser additive manufacturing of Zn metal parts for biodegradable applications: processing, formation quality and mechanical properties. Mater Des 155:36–45. https://doi.org/10.1016/j.matdes.2018.05.057

231. Delsmann MM, Sturznickel J, Kertai M et al (2022) Radiolucent zones of biodegradable magnesium-based screws in children and adolescents—a radiographic analysis. Arch Orthop Trauma Surg 143(5):2297–2305. https://doi.org/10.1007/s00402-022-04418-0

232. Wang JL, Xu JK, Hopkins C et al (2020) Biodegradable magnesium-based implants in orthopedics—a general review and perspectives. Adv Sci 7(8):1902443. https://doi.org/10.1002/advs.201902443

233. Herber V, Labmayr V, Sommer NG et al (2022) Can hardware removal be avoided using bioresorbable Mg-Zn-Ca screws after medial malleolar fracture fixation? Mid-term results of a first-in-human study. Injury 53(3):1283–1288. https://doi.org/10.1016/j.injury.2021.10.025

234. Luo Y, Zhang C, Wang J et al (2021) Clinical translation and challenges of biodegradable magnesium-based interference screws in ACL reconstruction. Bioact Mater 6(10):3231–3243. https://doi.org/10.1016/j.bioactmat.2021.02.032

235. Karunakaran R, Ortgies S, Tamayol A et al (2020) Additive manufacturing of magnesium alloys. Bioact Mater 5(1):44–54. https://doi.org/10.1016/j.bioactmat.2019.12.004

236. Li Y, Zhou J, Pavanram P et al (2018) Additively manufactured biodegradable porous magnesium. Acta Biomater 67:378–392. https://doi.org/10.1016/j.actbio.2017.12.008

237. Liu Y, Yang YQ, Mai SZ et al (2015) Investigation into spatter behavior during selective laser melting of AISI 316L stainless steel powder. Mater Des 87:797–806. https://doi.org/10.1016/j.matdes.2015.08.086

Authors and Affiliations

Wenbo Yang[1] · Hao Chen[1] · Haotian Bai[1] · Yifu Sun[1] · Aobo Zhang[1] · Yang Liu[1] · Yuchao Song[2,3] · Qing Han[1] · Jincheng Wang[1]

✉ Qing Han
my.hanqing@163.com

✉ Jincheng Wang
jinchengwangjlu@163.com

[1] Department of Orthopedics, Second Hospital of Jilin University, Changchun 130022, China

[2] College of Biological and Agricultural Engineering, Jilin University, Changchun 130022, China

[3] School of Materials Science and Engineering, Jilin University, Changchun 130022, China